Since January 2020 Elsevier has created a COVID-19 resource centre with free information in English and Mandarin on the novel coronavirus COVID-19. The COVID-19 resource centre is hosted on Elsevier Connect, the company's public news and information website.

Journal of Hazardous Materials 402 (2021) 123535

Contents lists available at ScienceDirect

Journal of Hazardous Materials

journal homepage: www.elsevier.com/locate/jhazmat

Review

Inorganic nanoparticles for reduction of hexavalent chromium: Physicochemical aspects

Zahoor H. Farooqi [a,*], Muhammad Waseem Akram [a], Robina Begum [a,*], Weitai Wu [b], Ahmad Irfan [c,d]

[a] Institute of Chemistry, University of the Punjab, New Campus, Lahore, 54590, Pakistan
[b] State Key Laboratory for Physical Chemistry of Solid Surfaces, Collaborative Innovation Center of Chemistry for Energy Materials, The Key Laboratory for Chemical Biology of Fujian Province, and Department of Chemistry, College of Chemistry and Chemical Engineering, Xiamen University, Xiamen, Fujian, 361005, China
[c] Research Center for Advanced Materials Science, Faculty of Science, King Khalid University, Abha, 61413, Saudi Arabia
[d] Department of Chemistry, Faculty of Science, King Khalid University, Abha, 61413, Saudi Arabia

ARTICLE INFO

Editor: Xiaohong Guan

Keywords:
Hexavalent chromium
Water pollution
Chemical reduction
Metal nanoparticles
Nanocatalysis

ABSTRACT

Hexavalent Chromium [Cr(VI)] is a highly carcinogenic and toxic material. It is one of the major environmental contaminants in aquatic system. Its removal from aqueous medium is a subject of current research. Various technologies like adsorption, membrane filtration, solvent extraction, coagulation, biological treatment, ion exchange and chemical reduction for removal of Cr(VI) from waste water have been developed. But chemical reduction of Cr(VI) to Cr(III) has attracted a lot of interest in the past few years because, the reduction product [Cr(III)] is one of the essential nutrients for organisms. Various nanoparticles based systems have been designed for conversion of Cr(VI) into Cr(III) which have not been critically reviewed in literature. This review present recent research progress of classification, designing and characterization of various inorganic nanoparticles reported as catalysts/reductants for rapid conversion of Cr(VI) into Cr(III) in aqueous medium. Kinetics and mechanism of nanoparticles enhanced/catalyzed reduction of Cr(VI) and factors affecting the reduction process have been discussed critically. Personal future insights have been also predicted for further development in this area.

1. Introduction

Hexavalent chromium [Cr(VI)] has hazardous effects on organisms and its removal from soil and water bodies has gained a considerable attention in last few decades (Zhou et al., 2016; Veerakumar et al., 2017). Cr(VI) is known as highly toxic, non-biodegradable and cancer causing material. It is found as an environmental contaminant in soil, surface and ground water. Cr(VI) is a cause of various diseases in human beings like dermatitis, lung and nasopharynx cancer on inhaling (Costa and Klein, 2006; Katz and Salem, 1993). It is enlisted as one of the priority water pollutants by United State Environmental Protection Agency (USEPA). It is being used extensively in various fields including wood preservation, electroplating, finishing of metals, textile industry, leather tanning industry and stainless steel production because of its specific characteristics. That is why, Cr(VI) is present in industrial wastewater as pollutant. It is urgent to develop various methodologies for elimination of Cr(VI) from water bodies. Various methodologies such as adsorption (Ali and Gupta, 2006; Maponya et al., 2020), membrane filtration (Kaya et al., 2016), solvent extraction (Venkateswaran and Palanivelu, 2004), electrochemical precipitation (Sun et al., 2015), coagulation (Golbaz et al., 2014), bioremediation (Beller et al., 2013; Benazir et al., 2010), ion exchange (Xiao et al., 2016) and catalytic reduction (Saikia et al., 2017) in addition to some traditional strategies (Barrera-Díaz et al., 2012; Malaviya and Singh, 2011) based on reduction followed by precipitation have been employed for removal of Cr(VI) from aqueous medium. Although adsorption technology is an in-expensive and green methodology and does not involve formation of any side products. Multistep preparation of adsorbent and incomplete removal of Cr(VI) from aqueous medium are few main limitations of adsorption technology. In ion-exchange method of water purification, Cr (VI) ions present in water are exchanged with ions of another metal electrostatically held on exchanger. The incomplete removal of Cr(VI) ions is one of the main limitations of ion exchange methodology. Ultrafiltration is also used to remove Cr(VI) from aqueous medium but

* Corresponding authors.
E-mail addresses: zahoor.chem@pu.edu.pk, zhfarooqi@gmail.com (Z.H. Farooqi), robina.hons@pu.edu.pk (R. Begum).

https://doi.org/10.1016/j.jhazmat.2020.123535
Received 31 May 2020; Received in revised form 7 July 2020; Accepted 20 July 2020
Available online 25 July 2020

membrane fouling, high operational cost and re-contamination of water during backwashing are few drawbacks of ultrafiltration methodology. Bioremediation of Cr(VI) is an in-expensive and green methodology for removal of pollutants from water but Cr(VI) is not easily degradable by microbes. Moreover bioremediation is a time taking process. Chemical method like chemical reduction of Cr(VI) to Cr(III) is one of the economical approaches used for complete elimination of Cr(VI) from aqueous medium. Reduction of Cr(VI) is thermodynamically feasible but kinetically sluggish reaction. The rate of reduction of Cr(VI) can be increased by using some inorganic nanoparticles as reductants or catalysts. Reduction of Cr(VI) by inorganic nanoparticles is termed as enhanced reduction while reduction of Cr(VI) by some suitable reducing agent in the presence of inorganic nanoparticles (nano-catalysts) is known as catalytic reduction. The use of inorganic nanoparticles as reductants (Fazlzadeh et al., 2017; Lv et al., 2017; Qian et al., 2017; Su et al., 2016; Zhou et al., 2020) as well as catalysts (Lv et al., 2020; Shao et al., 2017; Zhang et al., 2018) for Cr(VI) reduction has become the subject of interest due to high efficiency, low cost, environment friendly approach, applicability on industrial scale and no harmful byproduct formation in comparison to organic matter where re-oxidation may occur (Wang et al., 2019). In this treatment, Cr(VI) is completely converted into Cr(III) which has low mobility as compared to Cr(VI) (Li et al., 2016a). Reduction product [Cr(III)] is one of the essential nutrients for organisms. Although inorganic nanoparticles based materials used for Cr(VI) reduction may have some toxic effects on aquatic life but the reduction of Cr(VI) has been usually carried out in the presence of monometallic and bimetallic nanoparticles of some noble metals like Pt, Pd and Ag which do not have any significant toxic effects on aqueous environment. However, monometallic and bimetallic nanoparticles of some non-noble metal like Ni and Co have some toxic effects on aqueous organisms but their concentration is usually kept low to avoid their toxic effects on aquatic life.

Various reviews on removal of Cr(VI) from aqueous medium are available in literature but present review is totally different from already published reviews (Barrera-Díaz et al., 2012; Cheung and Gu, 2007; Jobby et al., 2018; Miretzky and Cirelli, 2010; Maitlo et al., 2019; Wang et al., 2016). For example, Cheung and Gu (2007) presented an overview of mechanism of Cr(VI) detoxification by microorganisms and concluded that microorganisms may convert Cr(VI) to Cr(III). Therefore reduction of Cr(VI) by microorganism is not a part of present review. Two years ago, removal of Cr(VI) by biosorption and biotransformation has been reviewed by Jobby et al. (2018). Similarly Miretzky and Cirelli (2010) have reviewed removal of Cr(VI) and Cr(III) from aqueous solution by raw and modified lignocellulosic materials using adsorption methodology. To avoid repetition, removal of Cr(VI) by biosorbents or lignocellulosic based adsorbents has not been discussed in present review. Barrera-Díaz et al. (2012) have reviewed reduction of Cr(VI) by biological and electrochemical methods. Maitlo et al. (2019) have recently reviewed adsorptive potential of various types of nanomaterials for treatment of wastewater contaminated with Cr(VI) in term of their adsorption capacity, removal efficacy and partition coefficient. Photocatalytic reduction of Cr(VI) within the metal-organic framework has been reviewed by Wang et al. (2016). However detailed discussion on the reduction of Cr(VI) in the presence of nanoparticles (used as reductants or catalysts) was not a part of aforementioned reviews. That is why, we are going to review Cr(VI) reduction by inorganic nanoparticles (reductants or catalysts) without any discussion on electrochemical and biological reduction of Cr(VI). Versatile nanoparticles have been developed for reduction of Cr(VI) to Cr(III) but to the best of our knowledge, the progress of reduction of Cr(VI) in the presence of inorganic nanoparticles has not been reviewed in the academic literature.

In present work, we have reviewed reduction of Cr(VI) into Cr(III) using different inorganic nanomaterials as catalysts and reducing agents but main attention has been given to nano-catalyzed reduction of Cr(VI). Recent developments in methodologies adopted for synthesis, stabilization and characterization of nanoparticles reported for reduction of Cr (VI) has been presented.

The review is divided into various sections. Section 1 is an introduction of the topic. Classification of various nanomaterials documented for Cr(VI) reduction has been elaborated in section 2. Section 3 presents critical overview of synthesis and stabilization of nanoparticles used for Cr(VI) reduction. Summary of the characterization techniques is given in section 4. Chemistry of catalytic reduction of Cr(VI) by different reductants has been discussed in sections 5. Study of catalytic reduction using spectrophotometry has been described in section 6. Factors affecting catalytic reduction of Cr(VI) to Cr(III) have been discussed in section 7. Section 8 gives an overview of catalytic recycling. In the last section (section 9), personal perspective on future work is given as guidelines for new researchers.

2. Classification of inorganic nanoparticles reported for Cr(VI) reduction

A wide variety of inorganic nanoparticles has been utilized for reduction of Cr(VI). They have been classified here on the basis of their function, nature and morphology.

2.1. Classification of nanoparticles on the basis of their function

Inorganic nanoparticles may be classified into two different categories on the basis of their function/role in reduction of Cr(VI) to Cr(III). Some inorganic nanoparticles have ability to act as reducing agent to convert Cr(VI) to Cr(III). Zerovalent iron (Zhao et al., 2020), iron sulfide (Yu et al., 2020), iron oxide (Yi et al., 2020) and iron based bimetallic (Ruan et al., 2020) nanoparticles have been reported as reducing agents for reduction of Cr(VI) to Cr(III). Iron exists in low oxidation state in such kind of nanoparticles and is oxidized simultaneously during Cr(VI) reduction. Such kind of nanoparticles have poor stability over the time, particularly in aqueous or air medium. They are consumed in reduction process and cannot be recycled easily. Some inorganic nanoparticles do not directly involved in reduction process but speed up the reduction of Cr(VI) with some suitable reducing agent. Monometallic nanoparticles of Pd (Tripathi and Chung, 2020; Dorosti et al., 2020), Pt (Sivaranjan et al., 2020) and Ag (Chen et al., 2018a) and their bimetallic (Bao et al., 2020; Mahar et al., 2019) nanoparticles have been widely used as catalysts for reduction of Cr(VI) with some suitable reducing agent. Such kind of nanoparticles are relatively stable and can be easily recovered for their re-use in Cr(VI) reduction.

2.2. Classification on the basis of nature of nanoparticles

Inorganic nanoparticles reported for Cr(VI) reduction on the basis of their nature may be classified as metallic nanoparticles, non-metallic nanoparticles and iron sulfide nanoparticles. Metallic nanoparticles may be further classified as nanoparticles with reducing properties and nanoparticles with catalytic properties. Bimetallic nanoparticles is another class of metallic nanoparticles that may have two catalytic active components (Mahar et al., 2019) or one catalytic active component along with a reducing metal component (Shi et al., 2019). Detailed discussion on aforementioned nanoparticles is given below.

2.2.1. Metallic nanoparticles

Various monometallic and bimetallic nanoparticles have been used for Cr(VI) reduction to Cr(III). A brief overview of different metallic nanoparticles used for Cr(VI) reduction has been presented here.

Zerovalent iron (Fe^0) nanoparticles have been proven to be eco-friendly candidates for reduction of Cr (VI) into Cr (III). Use of Fe nanoparticles in Cr(VI) reduction has been widely reported in literature due to high abundance, low cost, easy availability and high reducing ability of iron metal (Fazlzadeh et al., 2017; Lv et al., 2017; Qian et al., 2017; Su et al., 2016; Zhou et al., 2020; Chen et al., 2018b). Zerovalent iron is oxidized to Fe^{2+}/Fe^{+3} in process of Cr(VI) reduction to Cr(III) and

then Fe(III) is co-precipitated with Cr(III). Fe^0 nanoparticles are superiors to bulk zerovalent iron due to their high reactive surface area as well as good injectability (Fu et al., 2013). But Fe nanoparticles are highly prone to aggregation which results in loss of their activity. Therefore, fabrication of Fe nanoparticles is necessarily followed by their stabilization to keep them active for their application in Cr(VI) removal from aqueous medium. Various stabilizing systems have been developed to stop aggregation of iron nanoparticles to be used in reduction of Cr(VI) into Cr(III) in aqueous medium. For example, Shao-Feng et al. (Shao-feng et al., 2005) have studied the removal of Cr (VI) from aqueous system using Fe^0 nanoparticles. Starch was utilized as stabilizer to avoid aggregation of Fe^0 nanoparticles to be utilized for reduction of Cr (VI) into Cr(III). Starch is a good stabilizer to stop aggregation of Fe nanoparticles but chances of oxidation of Fe nanoparticles cannot be totally eliminated. Similarly, Petala et al. (Petala et al., 2013) used Fe^0 NPs stabilized on mesoporous silica material known as MCM-41 for reduction of Cr(VI). This MCM-41 system was proved to be suitable candidate for stabilization of active Fe nanoparticles because of its porous structures with narrow pore size distribution. Bentonite supported Fe^0 nanoparticles have been used for Cr(VI) reduction to Cr(III) (Diao et al., 2016). Bentonite material does not only stabilize Fe nanoparticles but also enhances their reactivity towards Cr (VI) reduction. Role of bentonite in enhancement of reactivity of Fe nanoparticles towards Cr(VI) reduction is not clear and needs further investigation. Cr(VI) removal from waste water by chemical reduction method using zerovalent iron (ZVI) nanoparticles stabilized on multi-walled carbon nanotubes has been also reported (Lv et al., 2011). The nanocomposite made of ZVI nanoparticles and carbon nanotubes was found to be more active system in comparison to the un-supported ZVI nanoparticles and ZVI nanoparticles supported on activated carbon for Cr(VI) reduction. Fe nanoparticles can be supported and stabilized on multi-walled carbon nanotubes to obtain nanocomposite with excellent ability of reduction of Cr(VI) to Cr(III) but further work is needed to be carried out for understanding of mechanistic pathway of removal of Cr (VI) by the nanocomposite. Fe^0 nanoparticles supported on Fe_3O_4 have been also used for elimination of Cr(VI) from aqueous solutions by reduction method (Wu et al., 2009). In Fe_3O_4-supported Fe^0 system, Fe nanoparticles are attached on the surface of Fe_3O_4 particle and cannot aggregate with each other. Graphene is widely used supporting system of Fe^0 nanoparticles because of its high surface to volume ratio, low manufacturing cost and good mechanical strength in comparison to many of other supporting systems. Graphene nanosheets supported Fe^0 nanoparticles have been also utilized for the efficient elimination of Cr (VI) from water using chemical methodology (Li et al., 2016a). The immobilization of ZVI nanoparticles onto graphene nanosheets enhances their stability and ability of electron transfer. The reduction of Cr (VI) into Cr(III) by zerovalent iron nanoparticles is an in-expensive method but stabilization of iron nanoparticles in zerovalent state is a difficult job. Therefore a lot of efforts have been made to stabilize Fe^0 nanoparticles for Cr(VI) reduction using various stabilizing systems and readers are referred to literature for further studies (Fazlzadeh et al., 2017; Lv et al., 2017; Qian et al., 2017; Su et al., 2016; Zhou et al., 2020; Chen et al., 2018b; Fu et al., 2013; Shao-feng et al., 2005; Petala et al., 2013; Diao et al., 2016; Lv et al., 2011; Wu et al., 2009).

Pd is a noble metal and nanoparticles of Pd can be stabilized more easily in comparison to Fe nanoparticles using suitable stabilizing systems. Moreover Pd at nanoscale has an excellent potential to catalyze a large variety of chemical reactions including reduction of Cr(VI) (Nasrollahzadeh et al., 2020). Use of Pd nanoparticles have been extensively studied for reduction of Cr(VI) into Cr(III) but role of Pd nanoparticles is different from that of Fe nanoparticles. Fe nanoparticles are highly reactive and act as reductant in reduction of Cr(VI) and are oxidized from zero oxidation state to higher oxidation states (Fe^{+2} and Fe^{+3}) as described in section 2.1. However reduction of Cr(VI) in the presence of noble metal nanoparticles like Pd, an additional reducing agent is needed while noble metal nanoparticles act as catalyst to speed up the reduction of Cr(VI). Catalytic reduction of Cr(VI) using Pd nanoparticles stabilized by different supporting systems has been widely documented in literature (Veerakumar and Lin, 2020). For example, Omole et al. (2007) have reported palladium nanoparticles in *N,N*-dimethylformamide for catalytic reduction of Cr (VI) using formic acid as hydrogen source. The use of unsupported palladium nanoparticles as catalyst in Cr (VI) reduction is not an economical method of elimination of Cr(VI) because they are not only unstable, their recovery from reaction mixture for re-use is also difficult. To stop their aggregation, palladium nanoparticles were stabilized in polyamic acid to obtain recoverable and reusable catalytic system with excellent catalytic activity. Polyamic acid itself has some toxic effects. It is important to replace toxic stabilizers with some environmentally benign supporting materials. Recently activated carbon supported palladium nanoparticles have been stabilized by ingredients derived from garlic skin for reduction of hexavalent chromium with formic acid (Veerakumar et al., 2017). The detailed discussion on synthesis of Pd nanoparticles will be given in section 3. High catalytic efficiency of the system may be attributed to the immobilization of palladium nanoparticles on porous surface of activated carbon.

Pd nanoparticles can be incorporated in mesoporous metal oxides and then can be used as catalysts but poisoning of the catalyst surface and difficulty in recovery and reusability of the catalyst are problems associated to use of such kind of catalytic systems. To overcome above mentioned problems, catalyst can be used as a thin film made of porous metal oxide loaded with Pd nanoparticles. For example, Dandapat et al. (2011) has reported glass substrate immobilized mesoporous-Al_2O_3 thin film loaded with Pd nanoparticles as an efficient and recyclable catalyst for reduction of Cr (VI) to Cr (III). Porosity of the metal oxide facilitates the diffusion of reactants to the Pd surface and its benign nature makes this system environment friendly. Catalyst can be obtained using small amount of precursor salt. Moreover, immobilization of catalyst film on glass substrate makes this system easily recoverable and reusable. Oxides of metalloids may also be used as mesoporous support of Pd nanoparticles. The immobilizing ability and stability of Pd nanoparticles on the surface of metalloid oxide can be enhanced by amine-functionalization of oxide surface. For example, Celebi et al. (2016) has reported highly stable Pd NPs supported on amine-functionalized silica (SiO_2) for reduction of Cr(VI). The approach used for immobilization and stabilization of Pd nanoparticles on amine-grafted silica was simple but not environmentally benign. Stabilization of Pd nanoparticles using hydrophilic polymeric material as support is more facile and economical approach. Hydrophilic polymeric system does not only stabilize Pd nanoparticles but also enhances their dispersity in water to easily carryout reaction in aqueous medium. Stabilization of Pd nanoparticles within electro spun polyethyleneimine (PEI) and polyvinyl alcohol (PVA) nanofibers crosslinked with glutaraldehyde for reduction of Cr(VI) into Cr(III) in aqueous medium has been reported by Huang et al. (2012). Facile approach, easy handling, small nanoparticles fabrication with uniform size distribution, large inter-particle distance, good stability, excellent catalyst dispersibility in water, good recoverability, reusability and high efficiency with complete Cr(VI) conversion into Cr(III) are fascinating features of the designed catalytic system. Pd nanoparticles supported on various organic and inorganic stabilizing systems for reduction of Cr(VI) have been widely studied. It is not possible to discuss all reports in detail in this review. Therefore readers are referred to the literature for further study (Tripathi and Chung, 2020; Veerakumar and Lin, 2020; Sadik et al., 2014; Gao et al., 2018; Yang et al., 2014; Sadeghi et al., 2019).

Platinum nanoparticles have been also proved an efficient catalyst for Cr(VI) conversion to Cr(III). Pt nanoparticles can be easily stabilized using suitable stabilizing material. Pt NPs have excellent catalytic activity but their use as catalyst for reduction of Cr(VI) is not encouraged due to high cost of Pt metal. However few reports are available on use of Pt nanoparticles as catalyst in reduction of Cr(VI). For instance, Dandapat et al. (2017) have immobilized well dispersed Pt nanoparticles on

Bismuth oxyhalide-alumina composite film using ethanol as reductant and used resulting material as catalyst to convert Cr(VI) into Cr(III). The presence of Bismuth oxyhalide (BiOX) increases rate of reduction of Cr (VI) but role of BiOX in enhancement of rate of reduction of Cr(VI) is not clear. Although catalytic system was found to be recoverable and re-usable but recovery of catalyst from reaction mixture after completion of the reaction was difficult. Pt based catalytic systems having additional magnetic material can be easily recovered by using external magnetic field. For example, Mai et al. (2017) have developed uniform bifunctional Fe_3O_4/mesoporous silica core/shell system for fabrication of Pt NPs by reduction of Pt precursor in the internal channels for reduction of Cr(VI). The catalytic system was found to be separable by using external magnet due to presence of Fe_3O_4 as core within the system.

Silver nanoparticles have gained attention as catalysts for various reduction reactions (Begum et al., 2019, 2017; Naseem et al., 2019; Begum et al., 2016) but their utility as nano-catalyst for Cr(VI) reduction is limited (Chen et al., 2018a; Liu et al., 2016a). Low stability of Ag nanoparticles as compared to other noble metal (Pt and Pd etc.) nanoparticles may be one of the possible reasons behind this limitation. Silver nanoparticles cannot catalyze dehydrogenation of formic acid to produce hydrogen for Cr(VI) reduction. This is another reason of avoiding application of Ag nano-catalyst in reduction of Cr(VI) with formic acid. Silver oxide layer formation around Ag nanoparticles and their high rate of aggregation because of their high surface energy, are other reasons of avoiding their use as catalyst in Cr(VI) reduction. Moreover, toxic reducing agents and expensive capping agents are needed for fabrication and stabilization of silver nanoparticles respectively for their use in catalysis. Therefore only two reports are available on catalytic application of silver nanoparticles towards reduction of Cr(VI) to Cr(III) in aqueous medium (Chen et al., 2018a; Liu et al., 2016a). Chen et al. (2018a) have reported magnetic carbonized polydopamine spheres decorated with silver nanoparticles by pyrolysis without using any reductant. The resulted catalytic system was used as a magnetically recyclable catalyst for catalytic reduction of Cr(VI) into Cr(III) using formic acid as hydrogen source. Mechanism of silver nanoparticles catalyzed Cr(VI) reduction is different from Cr(VI) reduction occurring in the presence of Pt and Pd nanoparticles and will be discussed in section 5. Recovery of silver ions from waste water or soil for synthesis of silver nanoparticles and their use as catalyst for removal of toxic materials from water may result in two-fold environmental application. For example, Liu et al., (2016) extracted Ag^+ ions from aqueous medium by biomass and then converted Ag^+ ions into silver nanoparticles by pyrolysis of biomass without using any external reductant and capping agent during nanoparticles fabrication. The resultant hybrid material (Ag@Biochar) was utilized as catalyst for Cr(VI) reduction to Cr(III).

Nickel nanoparticles are well known for their catalytic potential towards different reactions but to the best of our survey, only few reports are available on their use in reduction of Cr(VI) to Cr(III) with formic acid (Zhu et al., 2019; Bhowmik et al., 2014; Akram et al., 2019). Although Ni is non-noble metal like Fe but it cannot reduce Cr(VI) without additional source of hydrogen. For example, Akram et al. (2019) have reported thermally expanded reduced graphene oxide (TERGO) decorated with nickel carbide-nickel nanoparticles (Ni_3C-NiNPs) to obtain (TER/Ni_3C-NiNPs) nano-catalytic system with excellent catalytic potential towards Cr(VI) reduction to Cr(III) in aqueous medium. No additional reducing agent and capping agent was used for nanocomposite fabrication. Graphene extended structure itself acts as stabilizer to stop aggregation of nickel nanoparticles. Good catalytic activity was attributed to the unique combination of Ni_3C-Ni NPs and TERGO. High conductivity, good adsorption ability, large surface area, porosity and specific electronic properties of reduced graphene extended structure also contribute in high catalytic activity of nickel nanoparticles. By inspiration of above mentioned supportive properties of reduced graphene oxide, Bhowmik et al. (2014) also fabricated highly stable nickel nanoparticles loaded in reduced graphene oxide and reported that RGO cannot only stabilize nickel nanoparticles without any additional capping agent but also makes the catalytic system easily recoverable. Nickel-reduced graphene oxide nanocomposite can effectively reduce Cr (VI) to Cr(III) in the presence of formic acid as reducing agent at room temperature

N-doped carbon material loaded with transition metal nanoparticles has gained attention as catalyst for various reduction reactions but its use in Cr(VI) reduction has been rarely reported. This material may be highly useful for reduction of Cr(VI) due to prevention of corrosion of metal, promotion of electron transfer because of modification of electronic structure of surface carbon layer upon N-doping and high catalytic activity of transition metal. Zhu et al. (2019) have reported 3D N-doped graphene carbon nanotube network loaded with nickel nanoparticles (Ni@N-CNTs/N-G) by using Nickel-metal organic frame work and melamine as precursors. The resulting hybrid material was utilized for rapid Cr(VI) reduction to Cr(III) with formic acid.

2.2.2. *Bimetallic nanoparticles*

Various monometallic nanoparticles reported for Cr(VI) reduction have been described in previous section (2.1.1). According to above discussion, noble metal nanoparticles have excellent catalytic activities towards reduction of Cr(VI) but expensive nature of their precursor salts limits their use as catalyst at large scale. Nanoparticles of non-noble metal like zerovalent iron are highly unstable. They may lose their activity as result of their aggregation or due to oxide layer formation around them during synthesis, storage or even during catalytic reaction (Petala et al., 2013; Diao et al., 2016). Fabrication of bimetallic nanoparticles for catalytic reduction of Cr(VI) gives solution of problems associated to catalysis by both noble and non-noble metal nanoparticles. Moreover catalytic activity of bimetallic nanoparticles has been found much higher than that of monometallic counterparts because of synergistic effect (Saikia et al., 2017). Variation in electronic interactions between re-hybridized metal orbital in a bimetallic nanoparticle also may be the cause of enhancement of catalytic activity (Vellaichamy and Periakaruppan, 2016). For example, mixing a small amount of another metal having catalytic potential such as Ni, Cu, Pt and Pd (more noble than Fe) to zerovalent iron to form bimetallic nanoparticles does not only give more stability to zerovalent iron but also increases the activity of the system. Zhou et al. (2016) have reported fabrication of Fe/Ni by chemical reduction of precursor salts of both metals with KBH_4 in ethanol. Resulting bimetallic nanoparticle system was used for reduction of Cr(VI) to Cr(III) in the presence of ultra-sound. Rate of reduction of Cr(VI) in the presence of Fe/Ni bimetallic nanoparticles was found to be much higher than that in the presence of individual monometallic nanoparticles under similar reaction conditions. Jiang et al. (2018) used Fe-Cu bimetallic nanoparticles supported on chitosan for removal of Cr (VI) from wastewater using chemical reduction methodology. The reducing ability of the bimetallic composite system (chitosan-Fe/Cu) was found to be much higher than that of zerovalent iron nanoparticles of same size in case of Cr(VI) reduction. The enhanced catalytic potential of Cu-Pd alloy nanoparticles was also explored by Saikia et al. (2017) for reduction of nitroaromatics and hexavalent chromium. Hexavalent chromium has also been effectively reduced with formic acid using Au-Ag bimetallic nanoparticles catalyst stabilized by reduced graphene oxide (Vellaichamy and Periakaruppan, 2016). The uniformly distributed high contents of metal nanoparticles within RGO sheets has significant impact on catalytic activity of the system (Li et al., 2018). Catalytic activity of bimetallic system may be further improved by using N-doped reduced graphene oxide as support. Li et al. (2018) have reported reduction of Cr(VI) by using Pt-Pd bimetallic nanoparticles supported on N-doped RGO. High catalytic performance of Pt-Pd bimetallic nanoparticles was attributed to synergistic effect as well as specific structure of N-doped RGO. Hu et al. (2017) have presented environmentally benign fabrication of Pt-Au nanospheres stabilized by theophylline at RGO with enhanced catalytic efficiency towards Cr(VI) reduction. Recyclable Pt-Pd nanoparticles stabilized on

procyanidin-grafted eggshell membrane have also been reported for the reduction of hexavalent chromium in literature (Liang et al., 2014). Pt-Pd nanoparticles were stabilized on polyphenol grafted eggshell membrane (ESM) for reduction of Cr(VI). ESM is an in-expensive and environmentally benign supporting system for stabilization of Pt-Pd bimetallic nanoparticles. Synthesis of bimetallic nanoparticles using ESM as support will be discussed in section 3.

2.2.3. Metal sulfide nanoparticles

Metal sulfides can also be used for reduction of Cr(VI). They are highly effective at their nanoscale levels. For example nanoscale iron sulfide (FeS) is highly useful for removal of Cr(VI) from water and soil. They do not only have good ability to extract Cr(VI) ions from soil/water by adsorption but are also good reductants. FeS nanoparticles stabilized by different supporting agents for reduction of Cr(VI) have attracted much attention of scientists due to formation of insoluble chromium precipitates during process of remediation which can be easily separated out (Wang et al., 2019; Lyu et al., 2017, 2018; Gong et al., 2016; Wu et al., 2017). So process of remediation involves three steps called adsorption, reduction and co-precipitation. Wang et al. (2019) have used chitosan supported FeS nanoparticles for in-situ removal of Cr(VI) from groundwater and saturated soil. The mechanism of removal of Cr (VI) from ground water by iron sulfide nanoparticles involves more than one steps including adsorption of Cr (VI) ions on the surface of FeS nanoparticles and reduction of adsorbed Cr(VI) ions followed by precipitation.

2.2.4. Non-metallic (metal free) nanoparticles

Metal free reduction of Cr(VI) to Cr(III) may be carried out but only two reports are available in literature on reduction of Cr (VI) catalyzed by non-metallic nanoparticles (Gong et al., 2015; Tripathi et al., 2018). For example Triphathi et al. (Tripathi et al., 2018) have reported fabrication of protein stabilized zerovalent sulfur nanoparticles with narrow size distribution and spherical shape using F. benghalensis leaf extract and applied them as catalyst for reduction of Cr(VI).

2.3. Classification on the basis of morphology of nanoparticles

Inorganic nanoparticles used for reduction of Cr(VI) may be classified as homogeneous, core-shell, yolk-shell and nanoparticles attached on surface of microspheres on the basis of their morphology. Simple monometallic nanoparticles have same composition throughout the structure and are made of a large number of atoms of the same metal. These nanoparticles may be treated as homogeneous nanoparticles. Similarly, non-metallic nanoparticles like sulfur nanoparticles or iron sulfide nanoparticles have also same composition throughout the particle dimension and are also termed as homogeneous inorganic nanoparticles. However sometimes, monometallic nanoparticles are attached on the surface of another nanomaterial. Resulting system as whole may be treated as heterogeneous system. For example Chen et al. (2018a) stabilized silver nanoparticles on the surface of carbonized polydopamine nanospheres filled with Fe_3O_4 nanoparticles for reduction of Cr (VI). Fe_3O_4 nanospheres have been also decorated with zerovalent iron nanoparticles for chemical reduction of Cr(VI) but system is not recyclable due to consumption of zerovalent iron in reduction of Cr(VI) (Wu et al., 2009). Similarly Pd nanoparticles decorated lignin based phenolic microspheres have been recently reported for Cr(VI) reduction to Cr(III) (Chen et al., 2020). Low amount of precursor and negligible diffusional barrier are the main advantages of use of such kind of morphology of catalytic systems. polystyrene-b-poly(4-vinylpyridine) nanospheres decorated with Pt nanoparticles (Pt@PS-b-PVP) shown in Fig. 1 (A) have been applied for reduction of Cr(VI). Detail of method of Pt nanoparticles fabrication will be described in section 3. Pd nanoparticles attached on outer region of Fe_3O_4 nanocubes encapsulated in a thin layer of N-doped carbon shell of cubical shape have been also documented for reduction of Cr(VI) (Tian et al., 2020). Shell does not only protect Pd nanoparticles from oxidation and agglomeration but also facilitates the electron transfer for speedy reduction of Cr(VI). Shell region of N-doped carbon is porous and does not significantly affects diffusion of reactant molecules to the catalyst surface. Iron-iron sulfide core-shell nanoparticles with Fe^0 core and FeS shell have been reported for reduction of Cr(VI). Cr(VI) ions are adsorbed on FeS shell surface to get reduce by Fe^{+2} and Fe^{+2} changes its oxidation state from +2 to +3 but F(III)-Cr(III) hydroxides are precipitated on the surface of core-shell nanoparticles to slow down the process of reduction of Cr(VI) to Cr(III) (Gong et al., 2017). Core-shell system with Fe^0 core and SiO_2 shell has been also used for reduction of Cr(VI) but in this system, zerovalent iron core acts as reductant and mesoporous SiO_2 shell protects iron nanoparticles from aggregation and oxidation but allows diffusion of reactant molecules from bulk to Fe nanoparticles through its porous structure (Li

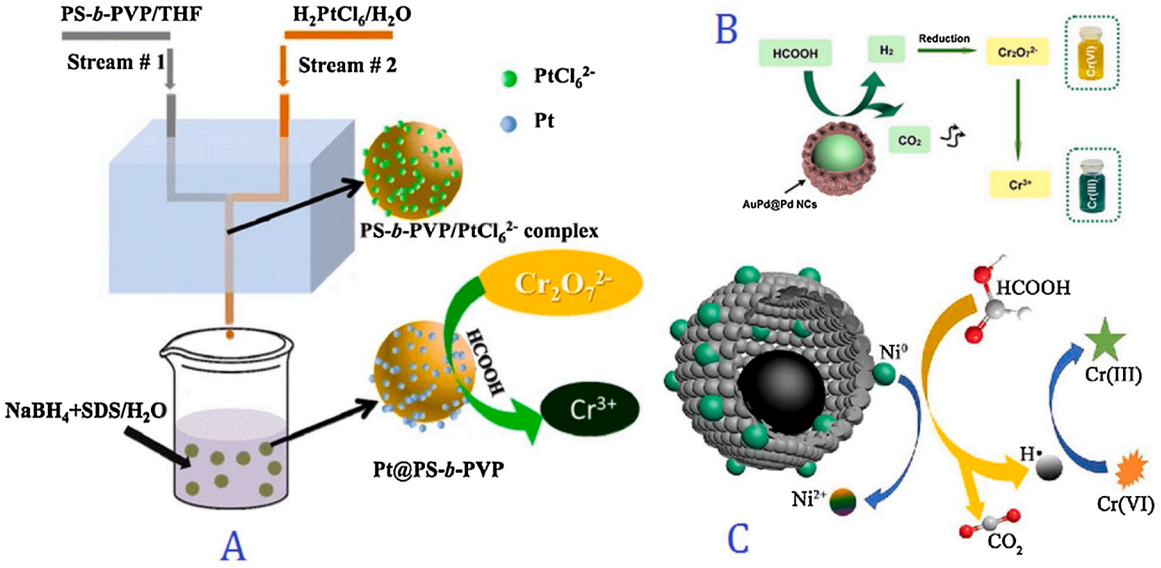

Fig. 1. Pt nanoparticles decorated on the surface of polystyrene-b-poly(4-vinylpyridine) nanospheres (Pt@PS-b-PVP) (A) adopted with permission from reference Zhang et al. (2018) (Copyright Springer 2018), Core-shell morphology of trimetallic nanoparticles with Au-Pd core and Pd shell (B) adopted with permission from reference (Shao et al., 2017) (Copyright Elsevier 2017), Nickel nanoparticles embedded carbon based yolk-shell system derived from Ni-MOF (C) adopted with permission from reference Lv et al. (2020) (Copyright Elsevier 2020) for Cr(VI) reduction to Cr(III).

et al., 2012). Similarly, bimetallic nanoparticles have atoms of two different metals in a nanoparticle. It is very difficult to get bimetallic nanoparticles with exactly uniform distribution of atoms of both metals throughout a nanoparticle. In case of nano alloys, atoms of both metals are present in the whole nanostructure but both metals have its own characteristics. Therefore, bimetallic nanoparticles cannot be treated as homogeneous nanoparticles. Bimetallic nanoparticles with different morphologies have been reported for reduction of Cr(VI). For example Au-Pd@Pd core shell catalytic system with Au-Pd alloy core and Pd shell have been fabricated by one-pot co-reduction methodology for highly efficient reduction of Cr(VI) in aqueous medium as shown in Fig. 1 (B) (Shao et al., 2017). Yolk-shell morphology is rare in nano-catalytic systems reported for reduction of Cr(VI) to Cr(III). Three-dimensional yolk-shell morphology of metal organic framework derived Ni-C system for reduction of Cr(VI) to Cr(III) has been recently reported by Lv et al. (2020) as shown in Fig. 1 (C).

3. Synthesis of nanoparticles for Cr (VI) reduction

Different inorganic nanoparticles including monometallic (Fe, Pt, and Pd, Ag and Ni), bimetallic (Fe-Ni, Pt-Pd, Pt-Au, Fe-Cu, Au-Ag etc.) and metal sulfide nanoparticles have been utilized for Cr(VI) reduction. Selection of method of fabrication of nanoparticles depends upon type of required nano-system. In general, two different methodologies (top down and bottom up approaches) are applied for the fabrication of all types of inorganic nanoparticles. The breaking of bulk material into nanoparticles by some mechanical means is known as top down approach while ions/atoms/molecules are combined together to form nanoparticles in bottom up approach (Petala et al., 2013; Hoeppener et al., 2002). Bottom up is superior because of easy control on shape, size and size uniformity of nanoparticles during their fabrication, low energy consumption and good dispersity and stability of nanoparticles in solvent. Most of the above mentioned nanoparticles have been fabricated using bottom approach. Naked inorganic nanoparticles are not stable because of their high surface energies. They may aggregate quickly to catalytically in-active bulk material. Therefore, synthesis of all type of inorganic NPs is carried out within the dispersion of some suitable stabilizer/support. Fabrication and stabilization of inorganic nanoparticles reported for Cr(VI) reduction has been described in the following sections in detail.

3.1. Synthesis of zerovalent iron nanoparticles

Fe° nanoparticles are usually fabricated by bottom up approach using some suitable stabilizing system. Starch, SiO_2, multi-walled carbon nanotubes, bentonite and magnetite (Fe_3O_4) are generally used as supporting materials for fabrication and stabilization of zerovalent iron nanoparticles (Fu et al., 2013; Shao-feng et al., 2005; Wu et al., 2009; Diao et al., 2016; Lv et al., 2011; Wu et al., 2009). Bentonite is extensively utilized as support for immobilizing zerovalent iron nanoparticles because of its high abundance, good chemical stability and excellent adsorption capability. Fe° nanoparticles supported on bentonite have been reported by Shi and co-workers (Shi et al., 2011) who used liquid-phase reduction approach for synthesis of zerovalent iron nanoparticles. $FeCl_3.6H_2O$ was dispersed in ethanol-water solvent system in the presence of required amount of bentonite. Sodium borohydride ($NaBH_4$) solution was injected into reaction vessel to reduce Fe(III) ions to zerovalent iron (Fe°) nanoparticles. Similarly synthesis of zerovalent iron nanoparticles in the inner surface of MCM-41 has been also reported using same reduction methodology with slight modification (Petala et al., 2013). For this purpose, ferric chloride ($FeCl_3{\cdot}6H_2O$) dissolved in ethanol was poured on the mesoporous material. The solvent was evaporated by heating the mixture at ~80 °C and resulting solid material was grinded into powder and dispersed into absolute ethanol to carry out reduction of iron salt by addition of sodium borohydride to obtain zerovalent iron nanoparticles. Fabrication of iron nanoparticles by chemical reduction method has been also reported in aqueous medium. For example, Lv et al. (2011) loaded Fe nanoparticles in multi-walled carbon nanotubes using chemical reduction of precursor salt in aqueous medium. Ferrous sulfate ($FeSO_4.7H_2O$) and carbon nanotubes were dispersed in deionized water by ultrasound and then $NaBH_4$ solution was injected into the mixture under N_2 purging and stirring to convert Fe^{+2} into Fe° according to the following reaction.

$$[Fe(H_2O)_6]^{+2} + 2BH_4^- \rightarrow Fe^0 + 2B(OH)_3 + 7H_2$$

Wu et al. (2009) used exactly same methodology of fabrication of zerovalent Fe nanoparticles in aqueous medium using Fe_3O_4 as stabilizer/support instead of carbon nanotube to get magnetically separable Fe nanoparticle based catalytic system.

In addition to chemical reduction of iron salt described above, microwave assisted synthesis (González-Arellano et al., 2008), decomposition of iron carbonyls (Vollmer and Janiak, 2011), decomposition of $\{Fe(N[Si(CH_3)_3]_2\}_2$ in the presence of hydrogen (Dumestre et al., 2004), thermal decomposition of Fe-metal organic framework (Zhang et al., 2016), chemical reduction of iron oxides (Hisano and Saito, 1998), vapor phase condensation (Stefaniuk et al., 2016), mechanical treatment (Ambika et al., 2016), method based on micro-organisms (Ravikumar et al., 2018), Laser ablation method (Okazoe et al., 2018) and carbo-thermal method (Wang et al., 2018) have also been reported for fabrication of iron nanoparticles but Fe nanoparticles prepared by these methods have not been reported yet for reduction of Cr(VI). Therefore, discussion on these methods is out of the scope of present review. Detailed discussion on method of synthesis of iron nanoparticles can be found in already published reviews (Stefaniuk et al., 2016; Zhao et al., 2016).

3.2. Synthesis of palladium nanoparticles

Palladium nanoparticles used as catalyst for Cr(VI) conversion to Cr (III) are usually synthesized by chemical reduction of palladium precursor using bottom up technique. For example Omole et al. (2007) have reported fabrication of palladium nanoparticles by chemical reduction method in non-aqueous solvent [N, N-dimethylformamide (DMF)] using palladium acetate as precursor. Palladium acetate was reduced with sodium borohydride in DMF at ambient temperature. Concentrated H_2SO_4 was added into stirred reaction mixture to form palladium colloidal particles. The un-reacted sodium borohydride was removed by microfiltration of acidified palladium colloid using water and DMF. Polyamic acid was used to stabilize Pd nanoparticles to be used as catalyst for Cr(VI) reduction to Cr(III). Dandapat et al. (2011) prepared Pd nanoparticles on mesoporous ɣ-Al_2O_3 film as a reusable catalyst for reduction of Cr(VI) to Cr(III). Mesoporous ɣ-Al_2O_3 film coated on glass substrate was dipped in $PdCl_2$ solution to load metal ions in it. Hydrogen-argon system (H_2/Ar) was used to reduce palladium salt into palladium nanoparticles. Pd-ɣ-Al_2O_3 film was used as catalyst for reduction of $K_2Cr_2O_7$ with formic acid. Same strategy of Pd nanoparticles fabrication has been reported by Celebi et al. (2016) who initially functionalized SiO_2 with amine groups by adding 3-aminopropyltriethoxysilane $[H_2N(CH_2)_3Si(OC_2H_5)_3]$ into ethanol containing SiO_2 and then reduced palladium(II) nitrate dihydrate $[Pd(NO_3)_2{\cdot}2H_2O]$ with sodium borohydride in aqueous medium to get Pd nanoparticles for reduction of Cr(VI). The donor-acceptor interactions between amino groups attached with SiO_2 surface and Pd nanoparticles give long term stability to Pd nanoparticles. Huang et al. (2012) used in-situ reduction approach for loading of catalytically active Pd nanoparticles on electrospun poly polyethyleneimine/polyvinyl alcohol (PEI/PVA) nanofibers. In this work, aqueous dispersion of PVA and PEI was electrospun and then crosslinking was caused by glutaraldehyde vapors to enhance the water stability of the system. Crosslinked nanofibers were loaded with potassium tetrachloropallidate (K_2PdCl_4). $[PdCl_4]^{-2}$ ions were diffused into the polymer matrix due to electrostatic attraction between

positively charged nitrogen of PEI and metal precursor anion. Then $NaBH_4$ solution was used to reduce Pd^{+2} into zerovalent Pd nanoparticles. The pictorial diagram describing the whole story of Pd nanoparticles fabrication in PEI/PVA matrix is shown in Fig. 2.

In all above schemes of Pd nanoparticles fabrication, $NaBH_4$ have been used as reducing agent which itself is highly toxic. To avoid the use of $NaBH_4$, chemical reduction may be replaced by thermal reduction but chemical reduction can be carried out at room temperature while thermal reduction needs high temperature. Veerakumar et al. (2017) have reported synthesis of Pd nanoparticles by thermal reduction and stabilized them by Garlic (*Allium sativum L.*) skin biomass. For this purpose, Garlic raw material was grinded, dried and then activated by mixing it with aqueous solution of zinc chloride in a Teflon-coated flask under microwave irradiation at 100°C. Resulting slurry was air dried at 100 °C and then it was graphitized in the presence of N_2 at 600−900 °C. Resulting carbonaceous material was cooled and washed with HCl. After pyrolysis at 400°C in CO_2 flow, the carbonaceous material (GAC) loaded with $PdNO_3$ was subjected to thermal reduction at 900°C in the presence of N_2 to obtain Pd@GAC.

3.3. Synthesis of platinum nanoparticles

Preparation of platinum nanoparticles (Pt NPs) using bottom up methodology for Cr(VI) conversion to Cr(III) has been reported in the presence of different supports (Dandapat et al., 2017; Mai et al., 2017). Dandapat et al. (2017) used bismuth oxyhalides (BiOX) to synthesize Pt nanoparticles within mesoporous Al_2O_3 in the form of a nanocomposite film. Ethanol was used as reducing agent to reduce metal ions into Pt nanoparticles in the presence of BiOX which acts as catalyst for oxidation of ethanol. In this way, metal ions can be successfully converted into metal nanoparticles without using any conventional reducing agent. Mai et al. (2017) fabricated Pt nanoparticles in bi-functionalized magnetic mesoporous silica using in-situ reduction method. The schematic illustration of fabrication of Pt nanoparticles in bi-functionalized Fe_3O_4/mesoporous silica core/shell nanoparticles is shown in Fig. 3. For preparation of Fe_3O_4/mesoporous silica core/shell structures, aqueous dispersion of Fe_3O_4 having triethanolamine (TEA) was charged with Tetraethyl orthosilicate (TEOS). Outer modification was carried out to functionalize SiO_2 shell surface with thiol groups (-SH). Then template was removed before inner modification for functionalization of inner surface with amine groups (-NH_2). Resulting Fe_3O_4@SH-SiO_2-NH_2 material was loaded with chloroplatinic acid hexahydrate ($H_2PtCl_6{\cdot}6H_2O$). Negatively charged $[PtCl_6]^{2-}$ ions were attracted by protonated amino groups (-NH_3^+) present in inner surface and repelled by negatively charged thiol group present on outer surface. As a result, $[PtCl_6]^{2-}$ ions are loaded on the inner side of channels. The inner surface with abundant –NH_2 group can chelate with metal ions by replacing chloride ions. After loading metal ions, sodium borohydride was added to reduce platinum ions into Pt nanoparticles as shown in Fig. 3. Zhang et al. (2018) have documented fabrication of Pt nanoparticles on the surface of polystyrene-b-poly(4-vinylpyridine) (PS-b-PVP) nanospheres using the technique of flash nanoprecipitation. For this purpose, PS-b-PVP/THF dispersion was mixed in a compartment with H_2PtCl_6/H_2O coming from different stream to load $[PtCl_6]^{2-}$into PS-b-PVP surface through chelation. $[PtCl_6]^{2-}$ ions attached on PS-b-PVP surface were then reduced to Pt nanoparticles using $NaBH_4$ as reductant in the presence of sodium dodecyl sulfate (SDS) as shown in Fig. 1 (A).

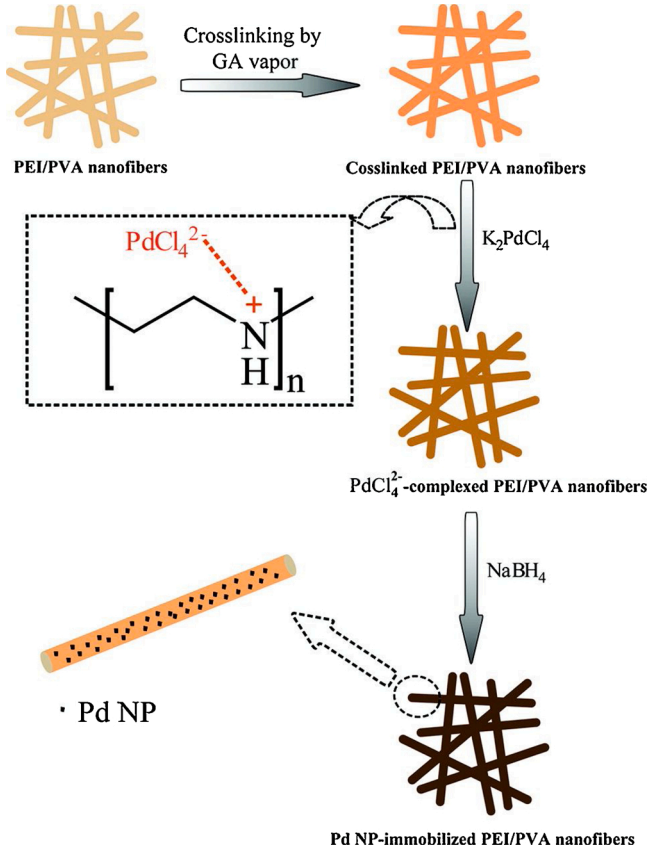

Fig. 2. Immobilization of palladium nanoparticles in electrospun polyethyleneimine and polyvinyl alcohol (PEI/PVA) nanofibers crosslinked by glutaraldehyde using in-situ reduction of K_2PdCl_4 with $NaBH_4$ in aqueous medium. Reproduced with permission from reference Huang et al. (2012). Copyright American Chemical Society 2012.

3.4. Synthesis of silver nanoparticles

Ag nanoparticles reported for catalytic reduction of Cr(VI), are synthesized by chemical reduction of silver salt usually silver nitrate. Chen et al. (2018a) have synthesized Ag nanoparticles based catalytic system for reduction of Cr(VI) into Cr(III) using chemical reduction approach. For this purpose, dopamine was self-polymerized in the presence of iron salt ($FeCl_3.6H_2O$) to obtain Fe-PDA complex and then silver nitrate solution was added to load silver ions on the surface of polydopamine complex spheres. Polydopamine acts as reductant to convert silver ions into silver nanoparticles. Heat treatment of silver nanoparticles decorated Fe-PDA spheres results in magnetic nanoparticles loaded carbonaceous material as shown in Fig. 4. The resulting hybrid material was used as magnetically separable catalytic system for Cr(VI) reduction to Cr(III) with formic acid. Chemical reduction approach for the fabrication of silver nanoparticles has been also reported by Liu et al. (2016a) who extracted silver ions from aqueous medium using fir sawdust (FSD) obtained from a local timber treatment plant as adsorbent. Biomass loaded with silver ions was subjected to pyrolysis in the presence of N_2 without adding any additional reducing agent and capping agent. Bio-oil was separated from resulting mixture and Ag nanoparticles loaded biochar was cooled and stored as solid residue for its further use as catalyst for Cr(VI) reduction to Cr(III).

3.5. Synthesis of nickel nanoparticles

Nickel nanoparticles were loaded on the surface of reduced graphene oxide by hydrothermal method using molecular hydrogen as reductant (Bhowmik et al., 2014). The schematic illustration of synthesis route is shown in Fig. 5. In the first step, graphene oxide (GO) was prepared and then GO was dispersed in aqueous solution of precursor salt ($NiCl_2{\cdot}6H_2O$) and hexamethylenetetramine by ultrasonic and then sealed in an autoclave for hydrothermal reaction for fabrication of Ni$(OH)_2$−GO at 120°C. Ni$(OH)_2$−GO composite was heated at 350 °C in the presence of H_2 under inert atmosphere of N_2 to get Ni NPs loaded on RGO sheets as shown in Fig. 5. Reduced graphene oxide does not only

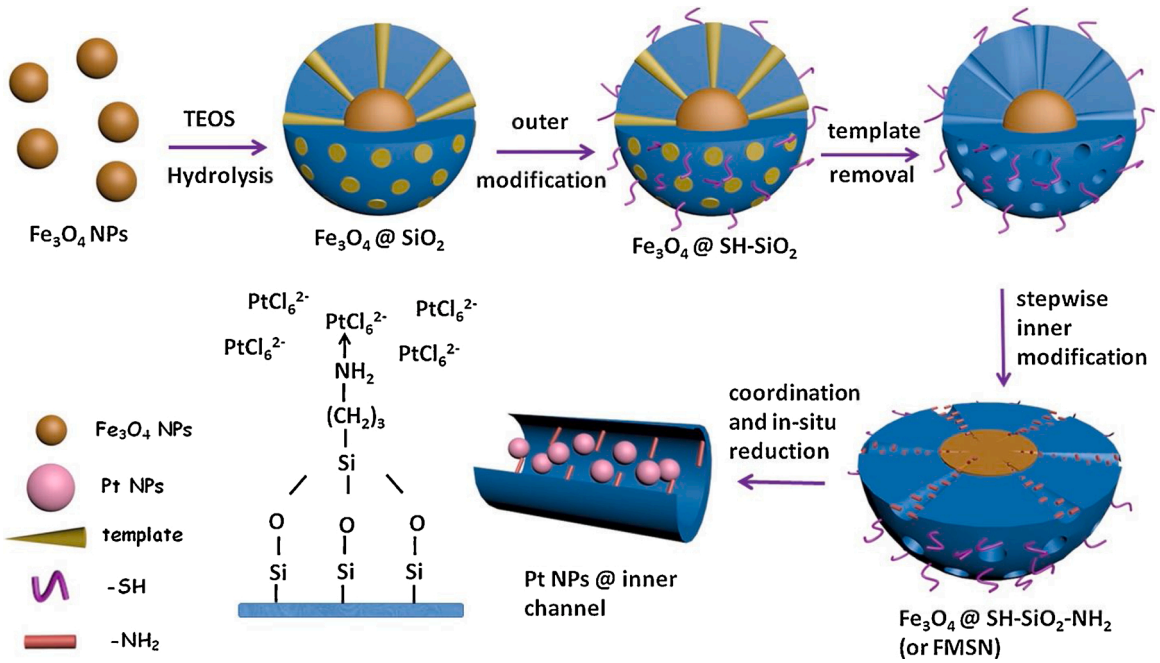

Fig. 3. Synthesis of platinum nanoparticles by in-situ reduction of $[PtCl_6]^{2-}$ with $NaBH_4$ in bi-functional Fe_3O_4/mesoporous silica core/shell nanoparticles (FMSNs) modified by thiol groups (-SH) on their outer surfaces and amine groups in their inner surfaces. Reproduced with permission from reference Mai et al. (2017). Copyright Elsevier 2017.

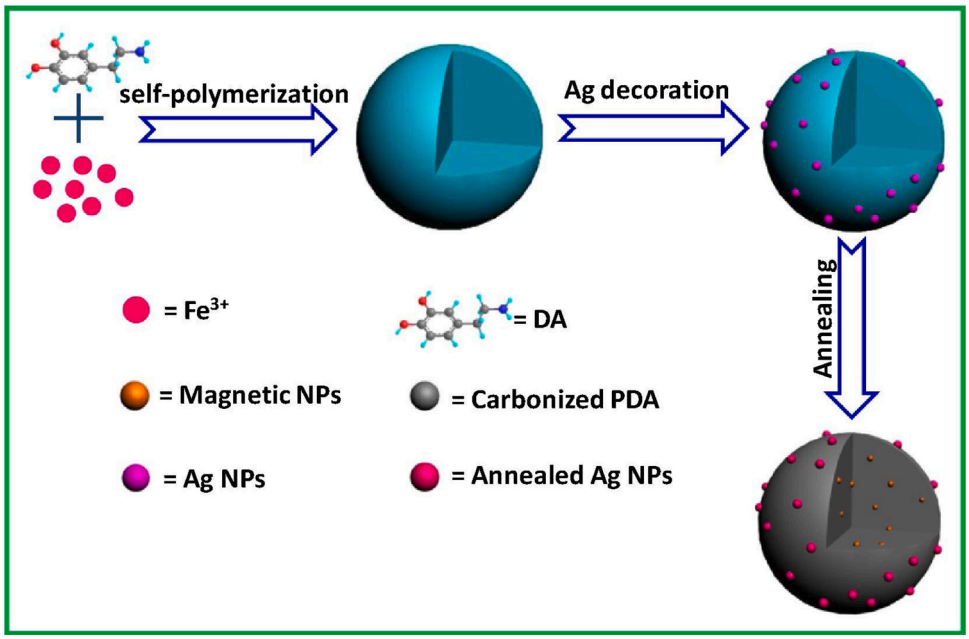

Fig. 4. Synthesis of silver nanoparticles decorated magnetic carbonized spheres obtained from self-polymerization of dopamine in the presence of iron salt. Reproduced with permission from reference Chen et al. (2018a). Copyright Elsevier 2018.

stabilize Ni nanoparticles but also enhances their catalytic activity towards reduction of Cr(VI). Fabrication and stabilization of Ni nanoparticles in the form of Ni_3C-Ni on thermally expanded reduced graphene oxide (TERGO) has been also reported by Akram et al. (2019).

Transition metal nanoparticles loaded into nitrogen doped carbon (M-N-C system) has gained attention as efficient catalysts for various reduction reactions. Nickel nanoparticles M-N-C catalytic systems have been used for this purpose because of their unique structure and surface properties. For example Zhu et al. (2019) have synthesized Ni-N-C system for reduction of Cr(VI). Ni-MIL and melamine were dispersed in ethanol and then reaction mixture was subjected to centrifugation to separate out solid material. Resulting solid material was initially pyrolyzed at 600 °C in the presence of argon and then heated at 800 °C to get Ni-N-C catalyst for reduction of Cr(VI).

3.6. *Synthesis of bimetallic nanoparticles*

Bimetallic nanoparticles utilized for reduction of Cr(VI) have been usually synthesized by chemical reduction method almost similar to the method described for synthesis of monometallic nanoparticles in

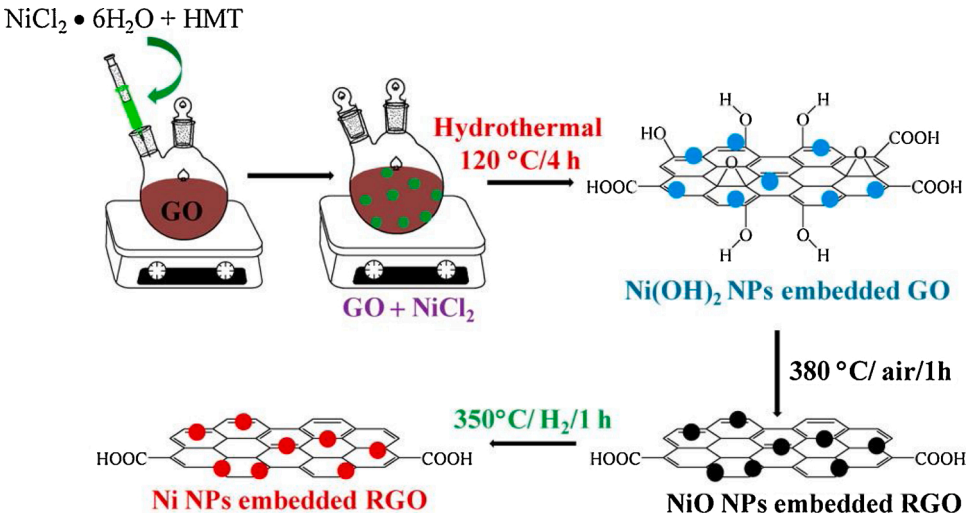

Fig. 5. Synthesis of nickel nanoparticles (Ni NPs) embedded in reduced graphene oxide (RGO) by hydrothermal method. Reproduced with permission from reference Bhowmik et al. (2014). Copyright American Chemical Society 2014.

previous sections. Although a wide variety of methods of preparation of bimetallic nanoparticles have been reported in literature but our discussion is limited to synthesis of those bimetallic nanoparticles that have been used for reduction of Cr(VI) (Peng et al., 2008; Sankar et al., 2012; Liu et al., 2014). Different attempts have been made into order to synthesize bimetallic nanoparticles based catalytic systems for reduction of Cr(VI). To the best of our knowledge, chemical reduction is one of the mostly reported methodologies. For example, Saikia et al. (2017) have prepared copper-palladium (Cu-Pd) bimetallic nanoparticles by simultaneous reduction of $CuCl_2.2H_2O$ and $PdCl_2$ using hydrazine as reducing agent in slightly basic pH medium in the absence of any external capping agent but the reduction process was carried out in aqueous medium at 120°C in an autoclave which is generally known as hydrothermal method. It is very difficult to store CuPd bimetallic nanoparticles without any stabilizing agent. Moreover use of CuPd based catalytic system for reduction of Cr(VI) is not cost effective due to presence of palladium metal in bimetallic system. Fabrication of bimetallic nanoparticles using precursors of in-expensive metals for Cr(VI) reduction is the best strategy. Zhou et al. (2016) have prepared cost effective iron-nickel (Fe-Ni) bimetallic nanoparticles for the removal of Cr(VI) from aqueous medium. Aqueous solution of KBH_4 was added to precursor salts of Ni and Fe ($NiSO_4.6H_2O$ and $FeCl_3.6H_2O$) dissolved in ethanol to carry out reduction of both metal ions to form Fe-Ni bimetallic nanoparticles at room temperature under N_2 atmosphere. It is almost impossible to stabilize Fe-Ni bimetallic particles for long time without strong capping agent because both metals especially on nanoscale are prone to oxidation/aggregation. Therefore freshly prepared Fe-Ni system has good activity for Cr(VI) reduction but cannot be stored for long time. Jiang et al. (2018) have prepared Fe-Cu bimetallic nanoparticles capped by chitosan with relatively better stability over the time for removal of Cr(VI) from waste water. Functionalities of chitosan like hydroxyl and amine groups bind with zerovalent metal nanoparticles to give them long term stability. $FeSO_4.7H_2O$ and $CuSO_4.5H_2O$ salts were simultaneously reduced with $NaBH_4$ in the presence of chitosan to obtain bimetallic nanoparticles with homogeneous distribution of atoms of both metals while core-shell Fe-Cu bimetallic nanoparticles with Fe core and Cu shell were obtained by step-wise reduction process. For synthesis of Fe-Cu core-shell system, Fe nanoparticles were initially synthesized by reduction of $FeSO_4.7H_2O$ with $NaBH_4$ in the presence of chitosan and then Fe nanoparticles were used as seed particles for fabrication of copper shell around Fe nanoparticles by reduction of $CuSO_4.5H_2O$ with same reducing agent in the same stabilizer. Size of core and thickness of shell can be controlled by controlling concentration of precursor salts. Colloidal stability of Fe-Cu bimetallic nanoparticles was found to be dependent on stabilizer contents. Aggregation of Fe-Cu nanoparticles can be controlled by chitosan but chances of oxidation cannot be totally avoided. Bimetallic nanoparticles made of two noble metals capped with suitable stabilizers can be easily stabilized for long term without oxidation. For example, Hu et al. (2017) have synthesized Au-Pt bimetallic nanoparticles by reducing H_2PtCl_2 and $HAuCl_4$ salts on reduced graphene oxide with hydrazine hydrate in theophylline simultaneously. Au-Pt bimetallic nanoparticles were found to be stable over the time and proved to have high activity for reduction of Cr(VI). Fabrication of RGO supported bimetallic nanoparticles for reduction of Cr(VI) has been widely reported in literature using same methodology as described above with slight modifications and can be found in recent literature (Vellaichamy and Periakaruppan, 2016; Li et al., 2018; Yao et al., 2020; Lu et al., 2017).

3.7. Synthesis of iron sulfide nanoparticles

Synthesis of FeS nanoparticles to be used for reduction of Cr(VI) is different from synthetic methods reported for metal nanoparticles. FeS nanoparticles reported for reduction of Cr(VI) are prepared by displacement reaction instead of reduction reaction in a suitable solvent under inert atmospheric condition. FeS nanoparticles are also unstable like above mentioned inorganic nanoparticles. Therefore, they are fabricated in the presence of a stabilizing system. Synthesis of FeS nanoparticles in the presence of various stabilizing agents has been widely reported in recent literature but general synthetic scheme is almost similar and has been described here (Wang et al., 2019; Yu et al., 2020; Lyu et al., 2017; Wu et al., 2017; Li et al., 2017; Wang et al., 2011; Tan et al., 2020). For example, Li et al. (2017) have reported synthesis of FeS nanoparticles using carboxymethyl cellulose (CMC) as stabilizer in aqueous medium by displacement reaction between $FeSO_4.7H_2O$ and Na_2S in aqueous medium under N_2 atmosphere. $FeSO_4.7H_2O$ solution was added into CMC solution at pH $\geq$ pKa of CMC (5.3) to form Fe^{2+}-CMC complex. Formation of Fe^{2+}-CMC complex was the result of donor-acceptor interaction between Fe^{2+} ions and COO^- groups of CMC. Then stoichiometric amount of Na_2S solution was added into dispersion of Fe^{2+}-CMC complex to form FeS nanoparticles as a result of electrostatic attraction between Fe^{2+} and S^{2-}ions. FeS nanoparticles were found stable over the time and were used for enhanced reduction of Cr(VI) in aqueous medium.

3.8. Synthesis of Non-metallic nanoparticles

Synthesis of non-metallic nanoparticles is different from that of

metallic nanoparticles. Our discussion is limited to synthesis of those non-metallic nanoparticles which have been reported for reduction of Cr (VI). Sulfur nanoparticles have been used as catalyst for reduction of Cr (VI) (Tripathi et al., 2018). Synthesis of sulfur nanoparticles is a subject of broad interest and has been reviewed in literature (Rai et al., 2016; Suleiman et al., 2013). Synthesis of sulfur nanoparticles used for Cr(VI) reduction has been discussed here. Tripathi et al. (2018) have reported biogenic synthesis of sulfur nanoparticles to be used as catalyst for reduction of Cr(VI). For this purpose, F. benghalensis leaf extract dispersion was added into sodium thiosulfate pentahydrate solution in deionized water. The precipitation reaction was initiated by addition of citric acid into the reaction mixture. Elemental sulfur nanoparticles were collected using the process of centrifugation and were found stable for catalytic reduction of Cr(VI). Various functionalities present in F. benghalensis leaf extract do not only act as capping agents but also are helpful in dispersing sulfur nanoparticles in aqueous medium.

4. Characterization techniques

Catalytic activity of inorganic nanoparticles towards reduction of Cr (VI) depends upon their nature, shape, size and size distribution and nature and morphology of the supporting material used. Therefore, a broad spectrum of techniques has been applied for the characterization of catalytic systems (inorganic nanoparticles along with stabilizers) used for the Cr(VI) reduction. The UV–vis spectrophotometry (UV–vis) (Tripathi et al., 2018; Kalwar et al., 2013), Fourier transform infrared spectroscopy (FTIR) (Lv et al., 2020; Tripathi et al., 2018; Kalwar et al., 2013), X-ray diffraction (XRD) (Shao et al., 2017; Chen et al., 2020), Transmission electron microscopy (TEM) (Lv et al., 2020; Zhang et al., 2018; Chen et al., 2020; Tian et al., 2020), Field emission scanning electron microscopy (FESEM) (Tian et al., 2020), dynamic light scattering (DLS) (Zhang et al., 2018), Thermogravimetric analysis (TGA) (Lv et al., 2020; Chen et al., 2018a; Tian et al., 2020), X-rays photoelectron spectroscopy (XPS) (Shao et al., 2017; Chen et al., 2018a, 2020; Tian et al., 2020; Wu et al., 2020), Atomic force microscopy (AFM) (Wu et al., 2020), Raman spectroscopy (RS) (Lv et al., 2020; Chen et al., 2018a; Wu et al., 2020), Brunauer Emmett-Teller (BET) (Lv et al., 2020; Chen et al., 2018a; Liu et al., 2016a), Magnetometeric analysis (MA) (Chen et al., 2018a) Elemental mapping (EM) (Chen et al., 2020) and scanning electron microscopy-energy dispersive spectrometry (SEM-EDS) (Shao et al., 2017; Wu et al., 2020) are frequently used for characterization as well as for investigation of catalysis process.

Theoretical details of characterization techniques used for analysis of inorganic nanoparticles is beyond the scope of this review. Only purpose of physical techniques used for characterization of inorganic nanoparticles without mathematical background has been described here. Catalysis is surface phenomenon and catalytic reduction of Cr(VI) needs surface to get reduce. Surface morphologies of the nanoparticles and their supports are investigated by SEM. Surface area of inorganic nanoparticles depends upon their surface to volume ratios. Shape, Size and size distribution of inorganic nanoparticles used for Cr(VI) reduction is measured by TEM. DLS is used for the same purpose in case of liquid dispersion of inorganic nanoparticles. UV–vis spectrophotometry has become a useful tool for characterization of noble metal nanoparticles and their use in catalysis. Size, size distribution and shape of Plasmonic nanoparticles may be predicted on the basis of UV–vis spectra of their dispersion. UV–vis spectrophotometry is widely used to monitor the progress of conversion of Cr(VI) to Cr(III). Catalytic reduction of Cr (VI) is affected by the ratio of content of catalyst to that of its support. Contents of true catalyst in composites are determined by AAS or ICP or EA. Metal nanoparticles used in catalytic reduction of Cr(VI) may change their oxidation state during reaction as a result of some reaction. The change in their oxidation state is confirmed by EDX and XPS. Information regarding oxidation state of catalyst and degree of crystallinity of inorganic nanoparticles is determined from XRD. The recoverability of catalyst by magnetic field is measured by magnetometry. Catalytic systems to be utilized for reduction of Cr(VI) should be stable in temperature window of the reaction and their stability as a function of temperature is judged by TGA. TGA is also useful for determination of content of inorganic material present in catalytic composite system. FTIR and Raman spectroscopies are used for investigation of interaction betweencatalyst and support of the catalyst. Porosity of the support and inorganic material plays a significant role in catalysis and is investigated by BET.

5. Chemistry of Cr(VI) reduction

Cr(VI) reduction to Cr(III) with various reducing agents has been reported in literature but our discussion is limited to only those reductants which have been used in inorganic particles induced/catalyzed reduction of Cr(VI). Mechanism of reduction depends upon nature of reducing agent and catalyst. Therefore chemistry of the reduction of Cr (VI) on the basis of reducing agent used has been divided into following sections.

5.1. Inorganic nanoparticles catalyzed Cr(VI) reduction

5.1.1. Cr(VI) reduction by formic acid/sodium formate

Cr(VI) reduction to Cr(III) catalyzed by inorganic nanoparticles is usually carried out using formic acid as reductant. Chemistry of catalytic reduction of Cr(VI) with formic acid depends upon nature of inorganic nanoparticles used as catalyst. There are two mechanistic possibilities of catalytic conversion of Cr(VI) on the surface of noble metal nanoparticles like Pt and Pd nanoparticles. In case of first possibility, formic acid molecules diffuse to Pd surface, get adsorbed and then get dehydrogenated into CO_2 and H_2. In-situ produced H_2 adsorbed on active sites of Pd acts as reducing agent and converts already adsorbed Cr(VI) to Cr(III). Cr(III) desorbs from catalyst surface and diffuses out from surface region to the bulk region. The schematic illustration of the above description is given in Fig. 6 A.

In the second mechanistic possibility, decarbonylation of formic acid occurs on the surface of Pd nanoparticles and CO and H_2O are produced as products in the first step. In the second catalytic step, CO adsorbed on Pd surface may act as reductant to convert Cr(VI) to Cr(III) on the surface of Pd nanoparticles as shown in Fig. 6 B. Second mechanistic possibility was ruled out by Li et al. (2016b) on experimental basis using Pd nanoparticles encapsulated in metal organic frame work (Pd-ZIF-67). In controlled experiments, catalytic Cr(VI) reduction to Cr(III) with commercially available H_2 under acidic conditions on the same catalytic system was found to be lower than that with in-situ produced H_2 under similar reaction conditions which reflected that in-situ produced H_2 is more reactive than commercially available H_2. Reaction was found to be very slow in case of reduction of C(VI) with external CO in the presence of same catalyst under same reaction conditions which eliminated the possibility of second mechanism. Therefore first possibility has been accepted as true mechanism of catalytic reduction of Cr(VI) with formic acid in the presence of Pd and Pt and has been reported in various publications (Liang et al., 2014; Li et al., 2016b; Yadav and Xu, 2013). For example, exactly same mechanism of catalytic reduction of Cr(VI) with formic acid in the presence of Pt metal nanoparticles has been reported by Mai et al. (2017) and has shown in Fig. 7. Formic acid is dehydrogenated into CO_2 and H_2 on Pt nanoparticle surface. H_2 is used to reduce $Cr_2O_7^{-2}$ to Cr(III) [See color change in reaction mixture from yellow to colorless in inset of Fig. 7]. Formation of Cr(III) from Cr(III) was confirmed by addition of sodium hydroxide solution into solution of product which was changed from colorless to green due to conversion of Cr(III) to $[Cr(H_2O)_6]^{+3}$ (See change in color in inset of Fig. 7). Omole et al. (2007) have reported same mechanism for Cr(VI) reduction with formic acid in the presence of palladium nanoparticles stabilized by polyamic acid. Reaction was not found to be occurred in the absence of any one of the catalyst and formic acid.

It is worth mentioning that mechanism of catalytic reduction of Cr

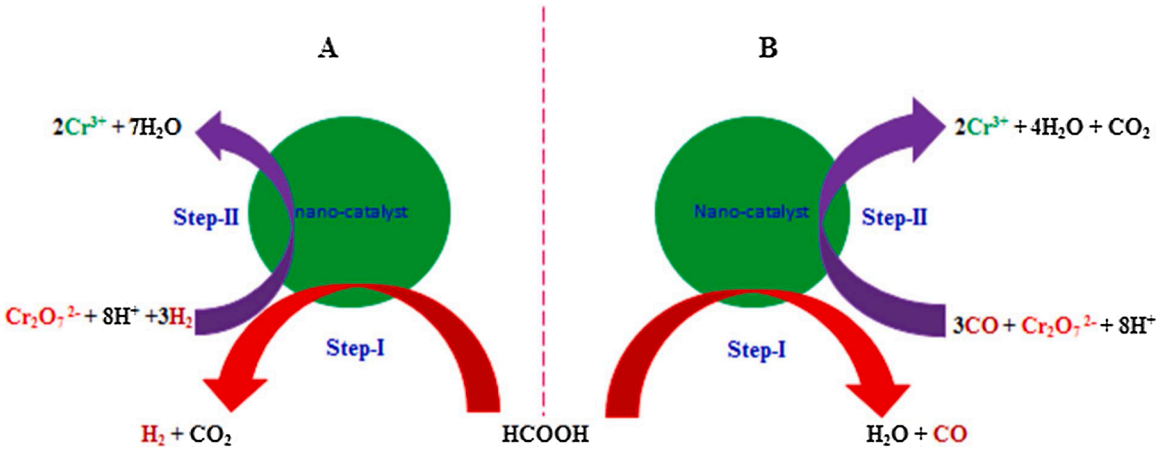

Fig. 6. Schematic illustration of two possible mechanisms of catalytic Cr(VI) reduction to Cr(III).

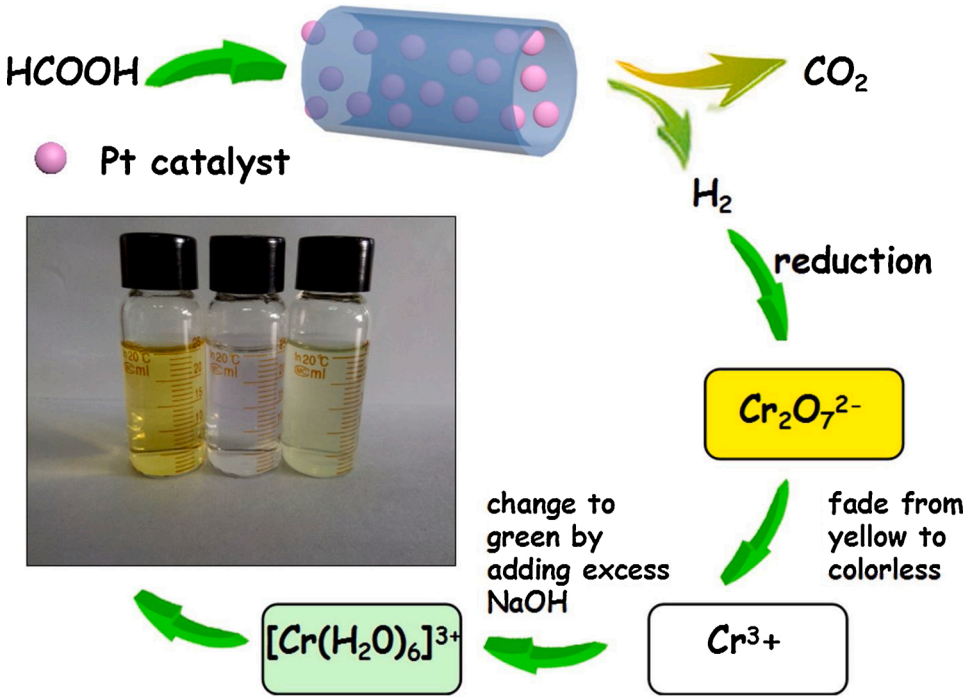

Fig. 7. Schematic illustration of mechanism of catalytic Cr(VI) reduction to Cr(III) with formic acid (HCOOH) using supported Pt nanoparticles. Reproduced with permission from reference Mai et al. (2017). Copyright Elsevier 2017.

(VI) with formic acid in the presence of silver nanoparticles is different from scheme described above. Dehydrogenation of formic acid cannot occur on the surface of silver nanoparticles. Therefore a different mechanism has been proposed for Cr(VI) reduction in the presence of silver nanoparticles (Chen et al., 2018a; Liu et al., 2016a). In catalytic reduction of Cr(VI), formic acid is initially decomposed into CO and H_2O on the surface of silver nanoparticles. Activated silver-carbonyl complex is generated as a result of activation of CO by silver nanoparticles which attracts Cr(VI) towards silver surface to form silver-carbonyl-Cr(VI) complex. In acidic medium, Cr(VI) in the complex is then reduced to Cr(III) with CO produced in first step through various intermediate transformations. A brief picture of the mechanism of silver nanoparticles catalyzed reduction of Cr(VI) with formic acid is given in Fig. 8.

Catalytic Cr(VI) reduction with H_2 was carried out in the presence of silver nanoparticles but no significant reaction progress was observed which signified that Cr(VI) reduction with H_2 cannot occurs in the presence of silver nanoparticles. Moreover in-situ produced CO was found to be more effective reductant in comparison to commercially available CO under similar conditions.

The mechanism of catalytic Cr(VI) reduction with formic acid in the presence of Au-Ag bimetallic nanoparticles is similar to that described for Ag catalyzed process in Fig. 8 but rate of reduction has been found to be higher in case of bimetallic nanoparticles (Vellaichamy and Periakaruppan, 2016) while Pt-Pd bimetallic catalyzed process follows mechanism of monometallic Pd catalyzed reduction of Cr(VI) as described above in Fig. 6 A.(Li et al., 2018; Hu et al., 2017). Reduction of Cr(VI) with formic acid in the presence of Au-Pd@Pd (Shao et al., 2017), Pt-Au (Hu et al., 2017), Cu-Ni (Borah et al., 2014), Pd-Cu (Trivedi et al., 2016) bimetallic nanoparticles is also occurred according to mechanism given in Fig. 6 B.

Kaining et al. (Gong et al., 2015) have reported molybdophosphate catalyzed reduction of Cr(VI) with formic acid via electron transfer but electron transfer mechanism in case of molybdophosphate catalysis needs further investigation and must be explored in future studies.

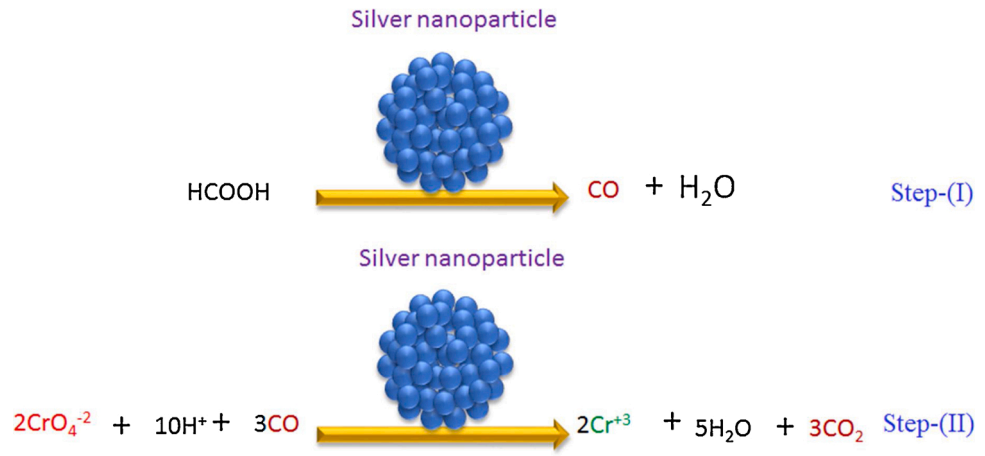

Fig. 8. Mechanism of catalytic Cr(VI) reduction to Cr(III) with formic acid (HCOOH) using silver nanoparticles as catalyst.

However in case of reduction of Cr(VI) with formic acid in the presence of non-noble metal nanoparticles, electron transfer mechanism has been proposed on the basis of experimental observations. Bhowmik et al. (2014) have reported redox mechanism of reduction of Cr(VI) using Ni nanoparticles supported on reduced graphene oxide in which formic acid adsorbed on Ni surface is initially decomposed to CO_2 and nascent hydrogen 'through redox process and oxidation state of nickel is changed from zero to +2. Surface atoms of nickel gets oxidized to NiO. Presence of NiO was confirmed by XRD and Raman analysis of recovered sample of the composite. The nascent hydrogen is highly reactive and reduces Cr (VI) to Cr(III).

Catalytic reduction of Cr(VI) with formic acid catalyzed by inorganic nanoparticles is one of the best strategies for removal of Cr(VI) from aqueous medium because of low toxicity, high stability and easy storage of reducing agent (formic acid). Formic acid also provides acidic medium which is favorable for reduction of Cr(VI). Moreover, no solid or liquid side product is formed in this process. Only CO_2 is produced during reduction reaction which may poison the surface of catalyst. But CO_2 is a gas and may be extracted from reaction mixture for useful purpose without releasing it into the atmosphere. Additionally formic acid is inexpensive and is available in local market.

Cr(VI) reduction to Cr(III) may be carried out using metal formate as hydrogen source. For example sodium formate (Li et al., 2016c; Yang et al., 2010) and mixture of formic acid and sodium formate (Celebi et al., 2016) has been reported as reductant for Cr(VI) conversion to Cr (III). Yang et al. (2010) reduced $K_2Cr_2O_7$ by sodium formate in the presence of viral templated Pd nanoparticles and reported that sodium formate acts electron donor in acidic environment. The chemical changes occurring during catalytic reduction of Cr(VI) by sodium formate under acidic condition may be summarized in the form of following ionic equations:

$$Cr_2O_7^{2-} + 14H_3O^+ + 6e^- \rightarrow 2Cr^{+3} + 21\ H_2O$$

$$HCOO^- + H_2O \rightarrow CO_2 + H_3O + 2e^-$$

5.1.2. Cr(VI) reduction by oxalic acid

Catalytic Cr(VI) reduction by oxalic acid in the presence of inorganic nanoparticles has been also reported in literature (Mahar et al., 2019) but mechanism of catalytic process is almost similar to that described in case of catalytic reduction of Cr(VI) with formic acid. Mahar et al. (Mahar et al., 2019) have recently reported Cr(VI) reduction by oxalic acid in the presence of Pt-Pd bimetallic nanoparticles supported on Indian tin oxide. It has been observed that oxalic acid is converted into H_2 and CO_2 on the surface of Pt-Pd nanoparticles. Nascent hydrogen produced acts as reducing agent to convert Cr(VI) into Cr(III) according to mechanism described in section 5.1 (Fig. 6).

5.1.3. Cr(VI) reduction by sodium borohydride

Sodium borohydride may be used as reducing agent for Cr(VI) reduction to Cr(III) in the presence of inorganic nanoparticles but Cr(VI) reduction by sodium borohydride has been rarely reported in literature. Toxicity, instability and basic nature of $NaBH_4$ are the major obstacles in its use as reductant for Cr(VI) reduction to Cr(III). Kalwar et al. (2013) have reported Cr(VI) reduction by sodium borohydride ($NaBH_4$) in aqueous medium in the presence of Ni nanoparticles stabilized by L-Cysteine. Catalytic Cr(VI) reduction to Cr(III) by sodium borohydride was monitored using UV–vis spectrophotometry by measuring the decrease in absorbance at 372 nm as a function of time. It is worth mentioning that usually catalytic Cr(VI) reduction to Cr(III) under acidic conditions is monitored by measuring the value of absorbance at 350 nm. $NaBH_4$ is basic in nature. Its addition to the mixture containing Cr (VI) increases the pH of the medium. As result, λ_{max} value of Cr(VI) is shifted from 350 nm to 372 nm due to conversion of $[Cr_2O_7]^{-2}$ to $[CrO_4]^{-2}$ before Cr(VI) conversion to Cr(III). Chemistry of catalytic Cr (VI) reduction to Cr(III) using Ni nanoparticles as catalyst has been described in the form of following chemical equation.

$$2K_2Cr_2O_7 + 2NaBH_4 \rightarrow 2Cr_2O_3 + 4KOH + 2NaOH + 2B\ (OH)_3$$

Non noble metal nanoparticles may lost their catalytic activity over storage due to their oxidation or aggregation. Utility of freshly prepared metal nanoparticles may result in an excellent catalytic efficiency. Loading of Cr(VI) into solution of metal precursor before nanoparticles fabrication leads to quick use of nanoparticles as catalyst for Cr(VI) conversion to Cr(III). For example Liu et al. (2016b) have reduced Cr(VI) by the addition of $FeCl_3$ and $NaBH_4$ into aqueous solution of $K_2Cr_2O_7$. According to their findings, zerovalent iron nanoparticles are produced by reduction of iron salt by sodium borohydride. In-situ produced Fe^0 nanoparticles have two fascinating features. They may act as catalyst to provide active sites for Cr(VI) reduction by $NaBH_4$. Zerovalent iron nanoparticles are highly reactive and may also act as reductant for Cr (VI) conversion to Cr(III).

Using aforementioned concept, reduction of Cr(VI) to Cr(III) by $NaBH_4$ in the presence of fly ash leachate (FAL) has been reported by Zhao et al. (2017). They reported that $NaBH_4$ reduces metal ions present in FAL to metal nanoparticles which act as catalyst for reduction Cr(VI) by $NaBH_4$. A comparison of catalytic reduction of Cr(VI) by formic acid and $NaBH_4$ in the presence of Ni nanoparticles supported on graphene oxide has been presented by Bhowmik et al. (Bhowmik et al., 2014) who reported that reduction ability of formic acid is much higher than that of $NaBH_4$ because reaction mixture has pH = 2 in case of Formic acid and pH = 7–8 in case of sodium borohydride. Cr(VI) reduction to Cr(III) is

highly pH dependent according to step-II of mechanism of catalytic Cr (VI) reduction given in Fig. 6 A.

5.1.4. Cr(VI) reduction by H_2

Pt, Pd and Pd-Pt nanoparticles catalyzed Cr(VI) reduction with formic acid discussed in section 5.1 describes that in-situ produced H_2 acts as reducing agent for Cr(VI) reduction. Therefore commercially available H_2 must be able to act as reductant in Pt/Pd nanoparticles catalyzed Cr(VI) reduction. The reduction must be carried out in acidic medium to fulfill the requirement of step-II of mechanism given in Fig. 6 A.

However silver nanoparticles are not good catalysts for efficient Cr (VI) reduction to Cr(III) due to poor adsorption of H_2 on the surface of silver nanoparticles. The Cr(VI) reduction ability of different reductants on the surface of silver nanoparticles reported by Liu et al. (Liu et al., 2016a) has been found in the order of HCOOH > CO>H_2.

5.1.5. Cr(VI) reduction by CO

Silver nanoparticles catalyzed Cr(VI) reduction with formic acid discussed in section 5.1 describes that CO produced acts as reducing agent for Cr(VI) reduction. Therefore commercially available CO gas can be used as reductant in inorganic nanoparticles catalyzed Cr(VI) reduction. The reduction must be carried out in acidic medium to fulfill the requirement of step-II of mechanism given in Fig. 8. Liu et al. (2016a) carried out Cr(VI) reduction with commercially available CO in the presence of H_2SO_4 on the surface of biomass stabilized silver nanoparticles. It was found that CO can reduce Cr(VI) to Cr(III) on the surface of silver nanoparticles but reduction efficiency was found to be low in comparison to in-situ produced CO (by dehydration of formic acid) under similar conditions. The same observation has been reported by Chen et al. (2018a).

5.2. Inorganic nanoparticles enhanced Cr(VI) reduction

5.2.1. Cr(VI) reduction by iron sulfide nanoparticles

Ferrous sulfide is a widely used material (both in bulk and nanoparticles forms) for remediation of Cr(VI) contaminated soil and ground water due to its good adsorbing ability and reducing power(Wang et al., 2019; Gong et al., 2016; Wu et al., 2017; Li et al., 2017). Our discussion is limited to the use of FeS nanoparticles as reductant for conversion of Cr(VI) to Cr(III). FeS nanoparticles are highly reactive in comparison to bulk FeS, due to their high surface to volume ratio and have gained considerable attention as active materials for Cr(VI) reduction in last few years (Lyu et al., 2017, 2018; Wu et al., 2017; Gong et al., 2017; Wu et al., 2020; Du et al., 2016; Chen et al., 2019). Chemistry of Cr(VI) reduction by FeS nanoparticles is simple. FeS nanoparticles do not only provide the surface for adsorption of Cr(VI) but also act as highly reactive reducing agent. Fe^{+2} is oxidized to Fe^{+3} by converting Cr(VI) to Cr(III) with simultaneous conversion of S^{-2} to SO_3^{-2}/SO_4^{-2}. Wang et al. (2019) have reported Carboxymethyl cellulose (CMC) stabilized FeS nanoparticles for reductive removal of Cr(VI) from ground water and soil. The schematic illustration of the process is shown in Fig. 9. FeS nanoparticles have ability to reduce adsorbed Cr(VI) as well as aqueous Cr(VI). The reduced [Cr(III)] and oxidized [Fe(III)] species both are precipitated in the form of their hydroxides in solid phase as shown in Fig. 9.

Gong et al. (2017) have reported adsorption of Cr(VI) followed by reduction and precipitation by FeS using core-shell nanoparticles with zerovalent iron core and FeS shell for Cr(VI) removal from ground water. Procedure of fabrication of FeS@Fe° core-shell nanoparticles is different from synthesis of FeS nanoparticles but mechanism of Cr(VI) removal from ground water is almost similar to that reported by Wang et al. (2019) and is shown in Fig. 10.

5.2.2. Cr(VI) reduction by iron nanoparticles

Cr(VI) reduction to Cr(III) by Fe° nanoparticles may be carried out without any catalyst and reductant. It is well known that zerovalent iron can reduce Cr(VI) to Cr(III) by forming Fe^{+2}. Recent investigations reveal that zerovalent iron cannot effectively act as direct reducing agent particularly in the pH range of 6.5–7.5 due to presence of oxide layer it in aqueous medium (Gheju, 2017, 2011; Gheju, 2018). The oxide layer around zerovalent iron nanoparticles is generally made of magnetite inner layer and hematite/maghemite outer layer. Direct transfer of electrons from Fe(0) to Cr(VI) is difficult due to presence of electron insulator outer layer around Fe(0). Moreover, oxide layer causes diffusional barrier against transfer of Cr(VI) from bulk region to Fe(0) surface. Under such pH conditions, removal of Cr(VI) from aqueous medium is mainly occurred by adsorption and indirect reduction with species like Fe^{+2} produced by Fe(0) corrosion. The Fe^{+2} ions have good potential to reduce Cr(VI) to Cr(III) by forming Fe^{+3}. Cr(VI) conversion to Cr(III) by both zerovalent iron and Fe^{+2} ions needs acidic conditions. Reduction ability of zerovalent iron nanoparticles is much higher than that of bulk iron because of their high surface to volume ratios. Therefore Cr(VI) reduction by Fe° nanoparticles is gaining attention day by day (Shang et al., 2017; Jin et al., 2018; Hu et al., 2019; Wang et al., 2017). Mechanistic pathway of Cr(VI) reduction to Cr(III) depends upon reaction conditions and may vary from condition to condition. A widely accepted general mechanism of Cr(VI) reductive removal by zerovalent iron nanoparticles reported in different

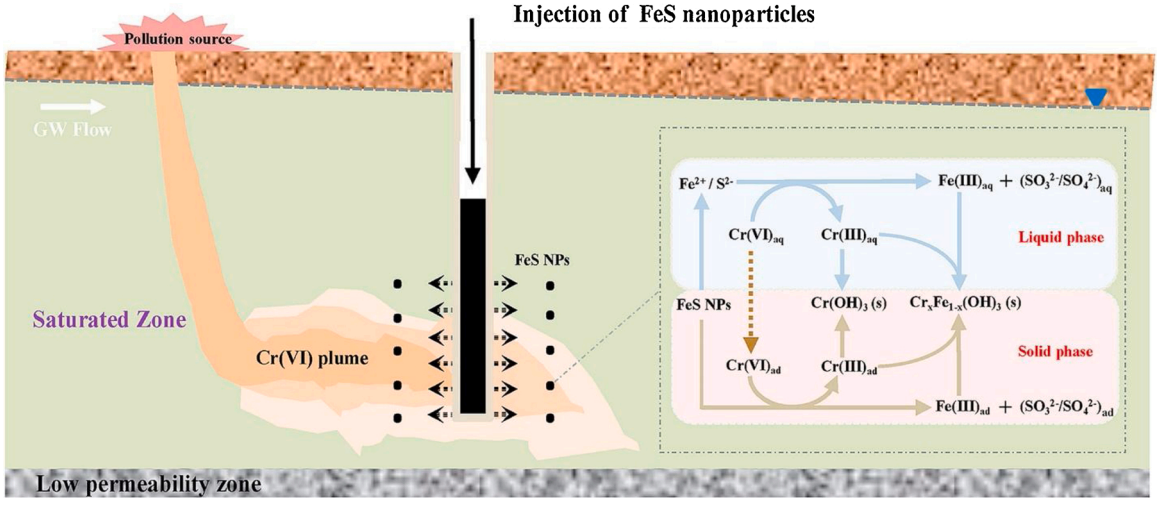

Fig. 9. Process of reductive removal of Cr(VI) from Soil using FeS nanoparticles as reductant. Reproduced with permission from reference Wang et al. (2019). Copyright Elsevier 2019.

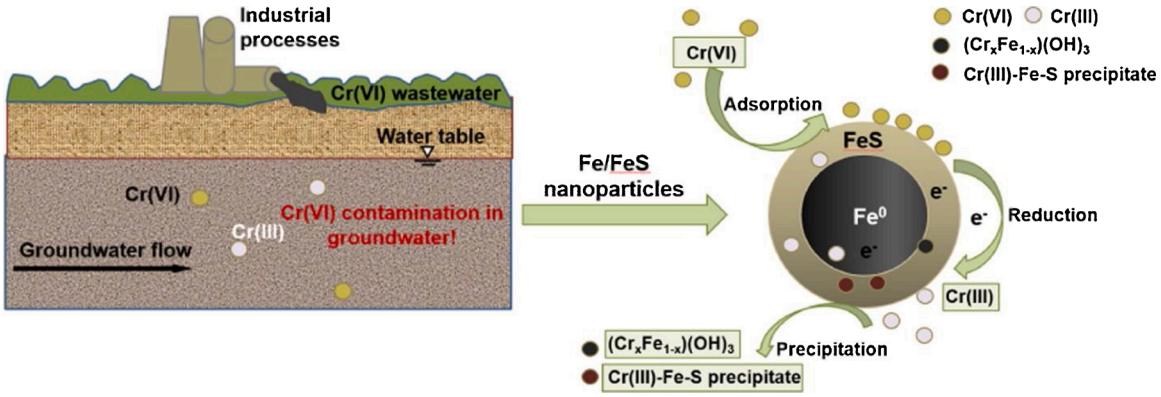

Fig. 10. Use of magnetic core-shell nanoparticles with zerovalent iron core and iron sulfide shell for Cr(VI) reductive removal from ground water. Reproduced with permission from reference Gong et al. (2017). Copyright Elsevier 2017.

publications (Jin et al., 2018; Lv et al., 2014, 2013; Zhang et al., 2019) has been described here. Cr(VI) is diffused from bulk region to surface of zerovalent iron nanoparticles and then get adsorbed on outer surface of iron nanoparticles. Adsorbed Cr(VI) is reduced to Cr(III) by Fe° nanoparticles while on the same time, Fe° is converted to Fe^{+2} in the presence of H^+. Fe^{+2} again acts as reductant for Cr(VI) conversion to Cr(III) with assistance of H^+. Redox reaction between Fe° or Fe^{+2} and Cr(VI) takes place on the surface of zerovalent iron nanoparticles. Iron oxide layer formation around Fe° nanoparticles may slow down the conversion of Cr (VI) to Cr(III). However oxide layer is porous and Cr(VI) still has chance to approach the surface of zerovalent iron nanoparticles. Cr(VI) reduction by Fe^{+2} results in production of Cr(III) and F(III) which are combined together in the form of hydroxides of Cr(III) and Fe(III) which are insoluble and co-precipitated on the surface of zerovalent iron nanoparticles. A significant retardation in Cr(VI) reduction to Cr(III) at later stages of the reaction has been observed due to complete Fe° surface coverage by Cr(III)-Fe(III) co-precipitates. Schematic illustration of widely accepted mechanism is given in Scheme 1.

5.3. *Inorganic nanoparticles enhanced and catalyzed Cr(VI) reduction*

Inorganic nanoparticles catalyzed reduction of Cr(VI) with some suitable reducing agent has been described in section 5.1 while Cr(VI) reduction by inorganic nanoparticles without any catalyst has been discussed in section 5.2. Section 5.2.2 reveals the self-retarding nature of Cr(VI) reduction by zerovalent iron nanoparticles. The electron transfer from Fe(0) to Cr(VI) becomes almost impossible due to coverage of iron surface by the reaction products [Fe(III)-Cr(III) (oxy)hydroxides]. Interestingly reducing metal nanoparticles may be coated with catalytically active metal to form bimetallic nanoparticles to overcome retardation process. Metals nobler than iron like Pd, Ag and Cu may be used for this purpose. Iron based bimetallic nanoparticles act as galvanic cell during Cr(VI) reduction to increase the reaction rate. Zerovalent iron nanoparticles act as reducing agents while noble metal act as electron transfer medium (catalyst) in process of Cr(VI) reduction that may be termed as inorganic enhanced and catalyzed Cr(VI) reduction. For example Hu et al. (2010) used Fe nanoparticles covered by copper layer for enhanced and catalyzed reduction of Cr(VI) in aqueous medium.

$$2HCrO_4^-(aq) + 3Fe^o(s) + 14H^+(aq) \rightarrow 3Fe^{2+}(aq) + 2Cr^{3+}(aq) + 8H_2O$$

$$HCrO_4^-(aq) + 3Fe^{2+}(aq) + 7H^+(aq) \rightarrow 3Fe^{3+}(aq) + 2Cr^{3+}(aq) + 4H_2O$$

$$xFe^{3+}(aq) + (1\text{-}x)Cr^{3+}(aq) + H_2O \rightarrow Cr_xFe(1\text{-}x)(OH)_3\downarrow + 3H^+$$

Scheme 1. Mechanism of Cr(VI) reduction to Cr(III) by zerovalent iron nanoparticles in aqueous medium.

They reported that combination of Cu (0) with Fe (0) does not only increase the Cr(VI) reduction rate but also increases the removal of Cr(VI) from aqueous medium per unit mass of Fe(0). The chemistry of the enhanced reduction process has been illustrated in Fig. 11. Cu(II) ions receive electrons from oxidation of Fe(0) and Fe(II) into Fe(II) and Fe (III) respectively for their own reduction and transfer them to Cr(VI) upon conversion of Cu(0) back to C(II) as shown in oxidation-reduction copper cycle of Fig. 11. Ni metal has behavior exactly similar to copper described above in case of Cr(VI) reduction in the presence of Fe-Ni bimetallic nanoparticles supported on montmorillonite (MMT) clay matrix reported by Kadu et al. (2011).

6. Study of catalytic reduction of hexavalent chromium

6.1. *Monitoring of catalytic reduction of Cr(VI)*

UV–vis spectrophotometry has become an excellent tool to monitor the progress of nano-catalyzed reaction (Begum et al., 2018a). It has been widely used to study the conversion of Cr(VI) into Cr(III) in the presence of inorganic nanoparticles (Wang et al., 2019; Gong et al., 2016; Wu et al., 2017) due to easy availability of the instrumentation and reliability of the results. Cr(VI) shows a characteristic absorption peak at 350 nm in acidic medium and at 372 nm in slightly basic medium (Kalwar et al., 2013). The decrease in value of absorbance corresponding to λ_{max} (350 or 372 nm) of Cr(VI) with time can be used to monitor the progress of conversion of Cr(VI) to Cr(III). There are two

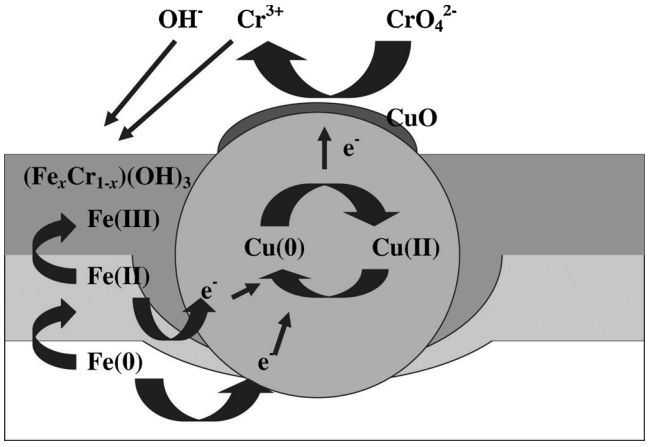

Fig. 11. Reduction of Cr(VI) to Cr(III) with zerovalent iron nanoparticles promoted by copper coated on Fe(0) nanoparticles in aqueous medium. Reproduced with permission from reference Hu et al. (2010). Copyright Elsevier 2010.

methods to monitor the catalytic reduction of Cr(VI) to Cr(III) by UV–vis spectrophotometry. First method is the scanning of spectra of a portion of reaction mixture taken from running catalytic reaction (outside the spectrophotometer) after specific time interval (Chen et al., 2020). In this method reaction is proceeded in separate vessel and sample is taken from the reaction vessel. The reaction mixture is filtered and diluted before spectrophotometric measurement. While in second method, the catalytic reduction reaction is carried out in a quartz cuvette placed with in spectrophotometer (Yang et al., 2010). In the later method, catalyst may interfere with Cr(VI) spectrophotometric measurement. However this interference can be minimized by using very low concentration of the catalyst in comparison to Cr(VI) concentration. Yang et al. (2010) has done a great job to eliminate interference of catalyst in case of in-situ monitoring of Cr(VI) reduction. They immersed specially designed Tobacco Mosaic Virus (TMV) template chips containing Pd nanoparticles in the inner walls of quartz cuvette for in-situ monitoring of catalytic reduction of Cr(VI) to Cr(III) without any interference of catalyst in spectrophotometric measurements because catalyst was not dispersed in reaction mixture. In both cases, time dependent UV–vis spectra of the reaction mixture is scanned in wavelength range of 200−600 nm. The value of absorbance at 350/372 nm decreases with time due to decrease in concentration of Cr(VI) because of its conversion into Cr(III). The extent of reduction of Cr(VI) is usually expressed in term of percentage conversion which is determined using the following formula (Yang et al., 2010).

$$Conversion(\%) = \left(\frac{C_o - C_t}{C_o}\right) \times 100 \quad (1)$$

Where Co is the initial concentration of Cr(VI) while Ct is the concentration of Cr(VI) at any time. Absorbance at λ_{max} of Cr(VI) is directly proportional to the Cr(VI) concentration in the reaction mixture. So C_o and C_t may be replaced by A_o and A_t respectively in expression (1) and percentage conversion can be measured by measuring value of absorbance of Cr(VI).The percentage conversion is plotted as a function of reaction time to measure the speed of reaction under different conditions.

6.2. Determination of rate constant (k_{app}) for Cr(VI) reduction

The activity of catalytic system is usually expressed in term of rate constant of the reaction. Pseudo first order kinetic model is used for determination of value of apparent rate constant for catalytic Cr(VI) reduction to Cr(III). The mathematical formulation of first order kinetic model in differential form can be formulated as:

$$-dC_t/dt = k_{app}\, C_t \quad (2)$$

Where $-dC_t/dt$ is the rate of change of Cr(VI) cocentration with respect to time, C_t is available Cr(VI) concentration at any time during the progress of the reaction and k_{app} is first order rate constant for Cr(VI) reduction to Cr(III). The concentration of reducing agent is kept much higher than that of Cr(VI) to fulfill the requirement of pseudo first order kinetic model. The value of apparent rate constant for catalytic Cr(VI) reduction is commonly determined from data of UV/VIS Spectrophotometric monitoring of the reaction using integrated form of Eq. (2) as given below

$$\ln(C_t/C_o) = -k_{app}\, t \quad (3)$$

Where C_t/C_o is the ratio of concentration of Cr(VI) at any time to its initial concentration and can be replaced by A/A_o according to Beer-lambert's law. So Eq. (3) is usually written in term of absorbance as given below.

$$\ln\left[\frac{A_t}{A_o}\right] = -k_{app}t \quad (4)$$

Where A_t and A_o indicates absorbance of Cr(VI) at any specific time (t) and initial time (t = 0) at λ_{max}. The value of k_{app} is determined from slope of plot of $\ln(A/A_o)$ versus time. The determination of k_{app} for catalytic Cr(VI) reduction in the presence of different catalytic systems has been reported by different groups (Shao et al., 2017; Huang et al., 2012; Vellaichamy and Periakaruppan, 2016; Wei et al., 2015; Ng et al., 2019). Monitoring of progress of Cr(VI) reduction and determination of rate constant can be easily understood by findings reported by Veerakumar et al. (2017) which are given in Fig. 12. Time dependent UV–vis spectra of catalytic Cr(VI) reduction to Cr(III) using formic acid as hydrogen source in the presence of different concentrations of the Pd nanoparticles based hybrid catalyst are given in Fig. 12 [from (a) to (c)]. The value of absorbance of Cr(VI) at its λ_{max} (350 nm) decreases with increase of time at each catalyst concentration due to Cr(VI) conversion into Cr(III). The insets of Fig. 12 [(a)-(c)] represent plot of $\ln(A/A_o)$ as a function of time for determination of rate constant at different catalyst concentrations. The value of k_{app} was found to be increased with increase of catalyst concentration. The change in color of reaction mixture from yellowish to colorless and then from colorless to greenish upon addition of excess NaOH into the mixture was an indication of Cr(VI) conversion to Cr(III) [Fig. 12 (d)].

7. Factors affecting the apparent rate constant (k_{app})

Cr(VI) is greatly affected by various factors including concentration of Cr(VI), catalyst and reductant, temperature and pH of the medium. Factors affecting the value of k_{app} have been discussed in following sections.

7.1. Effect of amount of catalyst on k_{app}

The value of apparent rate constant of the reaction is a function of Catalyst concentration and has been widely reported for various catalytic reactions (Naseem et al., 2018; Begum et al., 2018b, c) including reduction of Cr(VI) to Cr(III) (Zhu et al., 2019; Bhowmik et al., 2014). Catalyst provides active sites to the reactant molecules for adsorption. Adsorbed reactants are then converted into products on the surface of catalyst. The value of rate constant of reaction increases with increase in catalyst concentration due to increase of available active sites for adsorption of reactant molecules to be converted into products up to a particular extent and then becomes independent of catalyst concentration because after that point, available active sites become excessive in comparison to reactant molecules to be adsorbed. This observation of catalyst concentration dependence of k_{app} for reduction of Cr(VI) has been reported by various groups (Celebi et al., 2016; Zhu et al., 2019; Bhowmik et al., 2014). For instance, dependence of rate constant (k_{app}) on catalyst dose have been reported for catalytic Cr(VI) reduction in the presence of $Pd@SiO_2$-NH_2 (Celebi et al., 2016). The value of k_{app} was found to be increased with increase of Pd nanoparticles based catalyst dose which reflected that Pd based catalyst provided the surface for conversion of formic acid into CO_2 and H_2 to reduce Cr(VI) to Cr(III). Linear catalyst dose dependence of k_{app} followed by plateau in case of Cr (VI) reduction to Cr(III) in the presence of Ni nanoparticles supported on RGO has been reported in literature (Bhowmik et al., 2014).

7.2. Temperature effect on k_{app}

Catalytic Cr(VI) reduction is greatly affected by temperature of the medium. Temperature dependence of reaction is usually discussed by measuring the value of apparent rate constant (k_{app}) for catalytic Cr(VI) reduction as a function of temperature of reaction mixture. Temperature dependence of k_{app} is also used for determination Arrhenius constants (Pre-exponential factor and activation energy). The values of activation energy (E_a) and Pre-exponential factor (A) of catalytic reduction of Cr (VI) is computed from slope and intercept of the plot of $\ln(k_{app})$ versus 1/T using Arrhenius equation in its linear form given below.

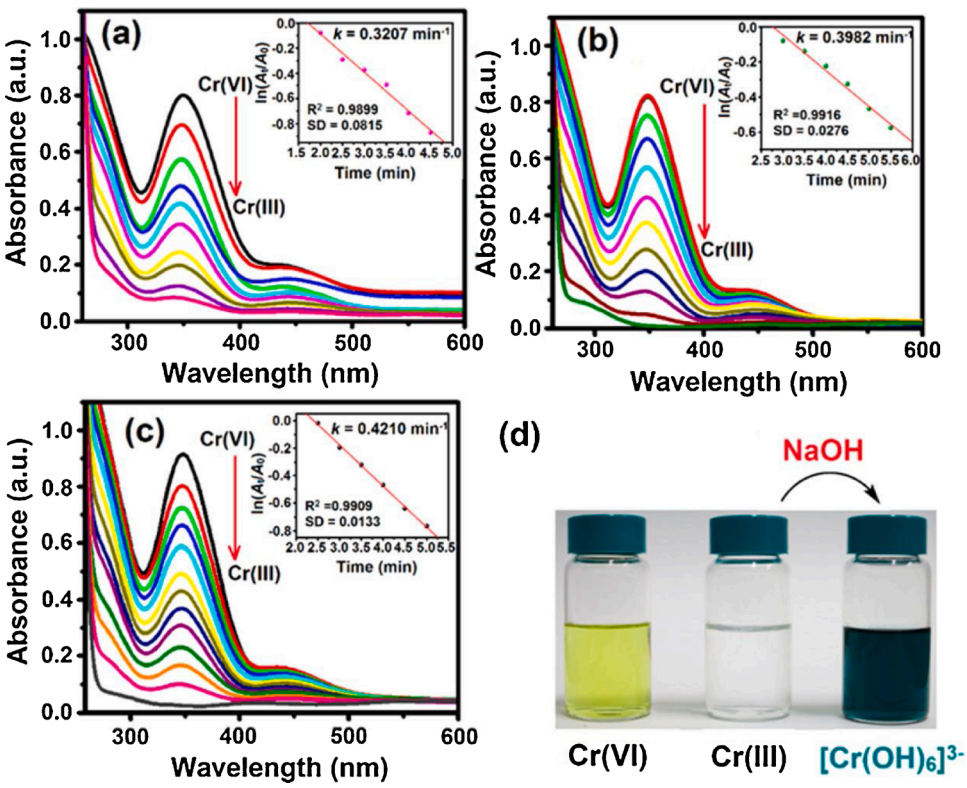

Fig. 12. Time dependent UV–vis spectra of reduction of Cr(VI) by formic acid (HCOOH) in the presence of biomass derived carbon stabilized palladium nanoparticles at different catalyst contents [(a) 0.50, (b) 1.00 and (c) 2.00 mg]. Insets of (a), (b) and (c) are plot of ln(A/A_o) vs time plots for determination of apparent rate constant at different catalyst loadings. Vials given in (d) represent sample before and after Cr(VI) reduction along with confirmation of Cr (III) by addition of sodium hydroxide. Reproduced with permission from reference Veerakumar et al. (2017). Copyright American Chemical Society 2017.

$$\ln k_{app} = -\frac{E_a}{R}\frac{1}{T} + \ln A \tag{5}$$

Temperature dependence of k_{app} for catalytic Cr(VI) reduction is also used for determination of thermodynamic activation parameters like entropy of activation (ΔS*) and enthalpy of activation (ΔH*). Value of ΔH*and ΔS* for catalytic Cr(VI) reduction are determined from slope of the plot of ln(k_{app}/T) versus 1/T according to Eyring equation given below.

$$\ln\left(\frac{k_{app}}{T}\right) = -\frac{\Delta H^*}{R}\left(\frac{1}{T}\right) + \ln\frac{k_B}{h} + \frac{\Delta S^*}{R} \tag{6}$$

Where R, k_B and h are gas constant, Boltzmann's constant and Plank's constant respectively. Celebi et al. (2016) have investigated the influence of temperature on the rate of catalytic reduction of Cr(VI) to Cr(III) by mixture of HCOOH and HCOONa in the presence of Pd nanoparticles on supported amine functionalized silica. The rate of Cr(VI) reduction was found to be increased with increase of temperature and data was found to be best fitted in Arrhenius and Eyring equation. Fig. 13 gives UV–vis spectra of catalytic Cr(VI) reduction after one minute [Fig. 13 (a)], plot of ln(C/C_o) versus time [Fig. 13 (b)], plot of ln(k_{app}) against 1/T [Fig. 13 (c)] and plot of ln(k_{app}/T) versus 1/T [Fig. 13 (d)] at five different values of temperature ranging from 298 to 318 K. Catalytic Cr (VI) reduction was carried out at five different values of temperature ranging from 298 K to 318 K. Linear relation between ln(k_{app}) and 1/T at different values of temperature predicted that temperature dependence of k_{app} for this reaction obeys Arrhenius equation. The value of activation energy was found 25.9 kJ/mol.

The values of E_a, ΔH* and ΔS* were found to be 25.9 kJ/mol, 30 kJ/mol and -158.7 J/mol.K respectively. The values of E_a, ΔH* and ΔS* for catalytic Cr(VI) reduction to Cr(III) depend upon reducing agent, size, morphology and nature of the catalyst and even stabilizing system and have been reported different in different publications (Dandapat et al., 2011; Yang et al., 2014). The values of Arrhenius and Eyring parameters for catalytic Cr(VI) reduction have been reported in different publications as described above but their physical significance to explore the insight of catalytic process has not been properly discussed in detail. Temperature dependence of k_{app} for catalytic Cr(VI) reduction by different reducing agents in the presence of different catalysts stabilized in various stabilizing systems may slightly deviate from above described pattern depending on experimental conditions and process technology and can be read in recent literature (Dandapat et al., 2011; Yang et al., 2014).

7.3. *pH effect on k_{app}*

The value of rate constant for catalytic Cr(VI) reduction is highly dependent on pH of the medium because H^+ ions are needed for Cr(VI) conversion to Cr(III) as shown in step–II of mechanism shown in Fig. 6. Addition of H^+ ions into the reaction mixture promotes Cr(VI) conversion to Cr(III). High concentration of H^+ needs acidic medium which can be achieved by decreasing the pH of the medium. Low pH of the medium is favorable for rapid Cr(VI) conversion to Cr(III) because at pH ≤ 2, Cr (VI) exists in the form of $HCrO_4^-$ which is more reactive than other forms of Cr(VI) like CrO_4^{2-} and $Cr_2O_7^{2-}$ that exist at pH > 2 (Tripathi et al., 2018). Mai et al. (2017) have reported catalytic reduction of Cr(VI) into Cr(III) by formic acid at pH = 2 and pH = 6 at 45 °C in the presence of Pt nanoparticles in aqueous medium. Rate of reduction was found to be much higher at pH = 2 than that at pH = 6. Similarly Li et al. (2016c) studied catalytic Cr(VI) reduction by oxalic acid at different pH values ranging from 2 to 7 under similar reaction conditions and reported pH = 2 as optimum pH for rapid conversion of Cr(VI) to Cr(III). Yao et al. (2020) have recently reported effect of pH of the medium on catalytic Cr (VI) reduction to Cr(III) with formic acid using RGO supported Cu-Ni bimetallic nanoparticles as catalyst and have found exactly same trend of pH dependence of reduction of Cr(VI). They also reduced Cr(VI) with different reducing agents including methanol (neutral), citric acid (pH = 1.0) and sodium borohydride (pH = 8) but formic acid (pH = 2) was found to be the best one because of its dual role in reduction process. It does not only act as reducing agent but also regulate the pH of the medium (nearly 2) for efficient Cr(VI) reduction.

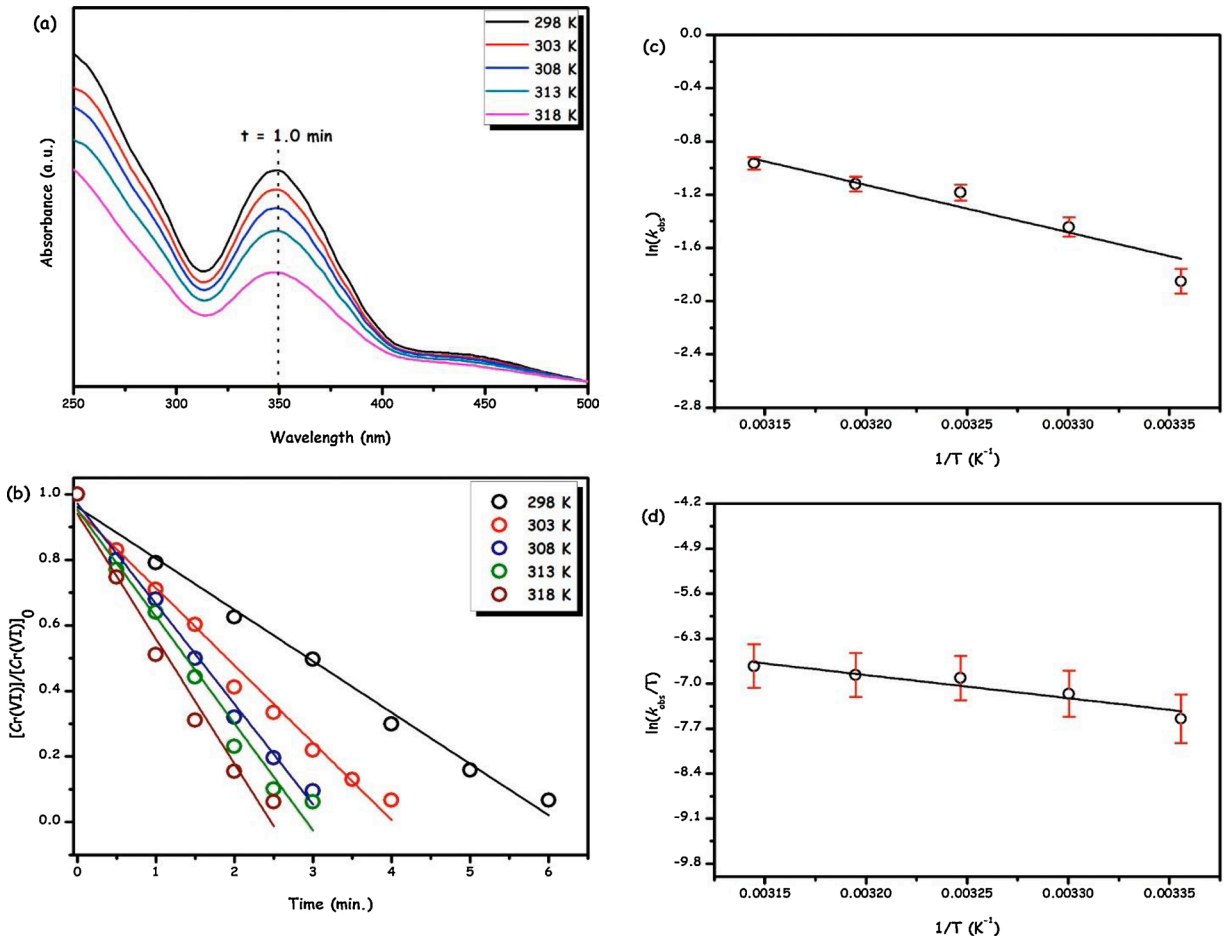

Fig. 13. UV Visible spectra of reaction mixture after one minute (a), plot of ln (C/C_o) versus time (b), Arrhenius plot (c) and Eyring plot (d) for catalytic Cr(VI) reduction to Cr(III) by mixture of formic acid and sodium format in the presence of Pd nanoparticles supported on amine functionalized silica at five different values of temperature in aqueous medium. Reproduced with permission from reference Celebi et al. (2016). Copyright Elsevier 2016.

7.4. Other factors affecting Cr(VI) reduction

Some other factors like nature of reducing agent, nature of supports used for stabilization of nano-catalysts, weight ratio of metal nanoparticles to supports, content of Cr(VI) and reducing agents may also affect the rate of reduction of Cr(VI) (Yao et al., 2020) but data reported on such kind of factors is limited and has not been discussed in this report. Role of such kind of factors is not much clear and needs further studies for optimization of process parameters to carry out reduction of Cr(VI) at large scale.

8. Catalyst recycling in reduction of Cr(VI)

It is highly important to recover nano-catalysts from reaction mixture after conversion of Cr(VI) to Cr(III). Recycling becomes necessary in case of use of nanoparticles of precious metals like Pt and Pd. The literature survey made by us to prepare this report reveals that recycling of catalytic systems can be achieved by centrifugation or by applying magnetic field (Dandapat et al., 2011). Recycling of nanoparticles by centrifugation is difficult because of their ultra-small size. Ultra-centrifugation is needed to recover nanoparticles from reaction mixture. However, immobilization of nanoparticles on solid support makes them easily recoverable catalysts at low round per minutes by ordinary centrifuge machine. Other tool of making recyclable inorganic nanoparticles based catalysts is to design a catalyst having magnetic nature or to add some additional magnetic material into the catalyst for their easy recovery from reaction mixture after completion of Cr(VI) reduction. The recovered catalyst must be able to do same function for the next cycle of the same reaction or some different reaction. In case of catalytic reduction of Cr(VI) to Cr(III), CO_2 (side product) and Cr(III) ions (product) may get adsorbed on the surface of nano-catalysts and may cause decrease in their activity for the next cycle. Therefore selection of materials to be used for nanocatalysts fabrication should be made on ability of catalysts to resist adsorption of CO_2, Cr(III) and any other possible impurity. Metal nanoparticles should be strongly stabilized by supporting system to avoid aggregation, oxidation and leaching during each cycle. Moreover, supporting materials of nanocatalysts should be able to afford harsh reaction conditions without any change in their morphology and functionality. Yao et al. (2020) reported recycling of reduced graphene oxide stabilized Cu-Ni bimetallic nanoparticles from Cr(VI) catalytic reduction mixture using external magnetic field. Catalyst was found to recyclable up to eight cycles without any significant loss of activity. However time required for complete Cr(VI) to Cr (III) conversion was found to increase with increase of cycle number. The slight decrease in catalytic activity of the system was attributed to oxidation of surface atoms of copper nanoparticles. Tian et al. (2020) have reported Fe_3O_4/Pd composite nanoparticles surrounded by nitrogen doped carbon shell as magnetically separable catalyst for Cr(VI) reduction to Cr(III) due to presence of Fe_3O_4. Decrease in activity of catalyst was attributed to formation of PdHX complex during catalytic Cr(VI) reduction to Cr(III). Pd nanoparticles supported on the surface of lignin based phenolic nanospheres have been recently reported by Chen et al. (2020) as recoverable catalysts for Cr(VI) reduction. Catalyst was recovered from reaction mixture through centrifugation, washed with

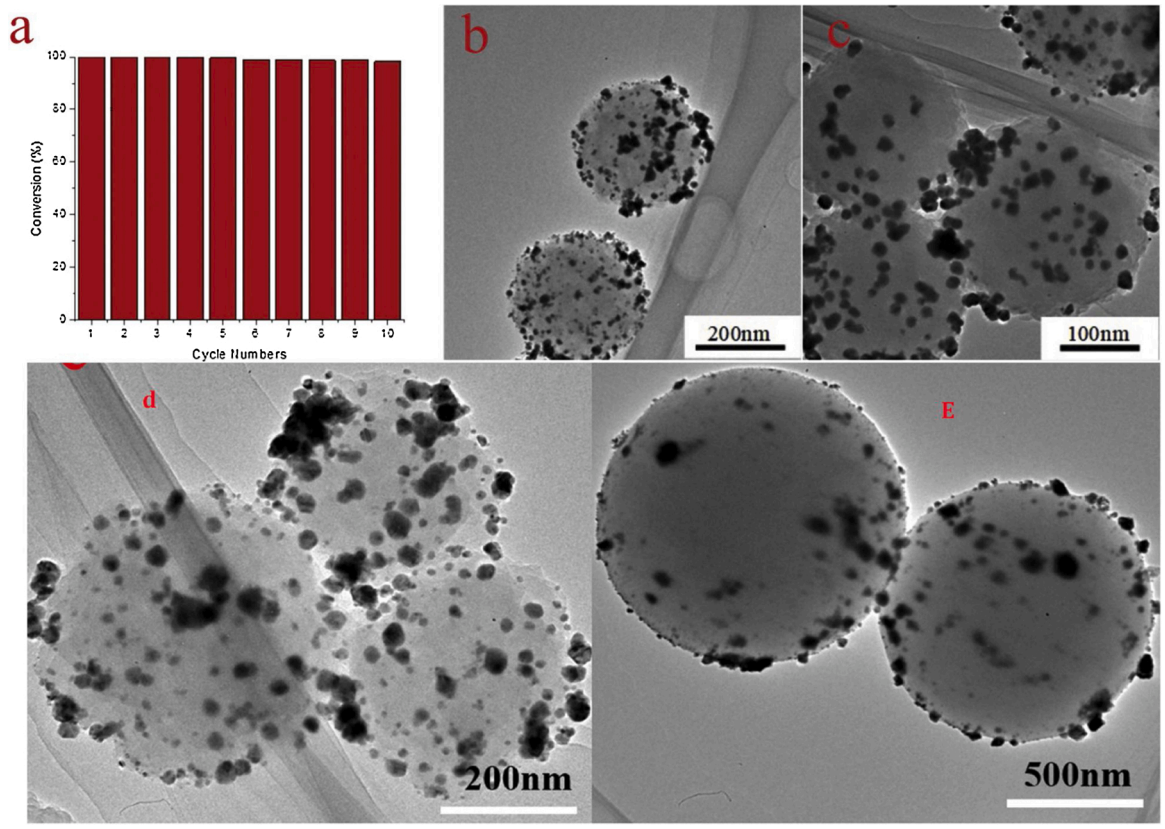

Fig. 14. Recycling of Pd nanoparticles supported on lignin based phenolic spheres in case of reduction of Cr(VI) (a), TEM images of recycled catalyst (b-c) and before their use as catalyst (d-e). Adopted with permission from reference Chen et al. (2020). Copyright Elsevier 2020.

ethanol, air dried and then was used for the next cycle. Catalyst was found to be recyclable without any loss of activity up to 10 cycles of reduction of Cr(VI). Data collected from recycling experiment is shown in Fig. 14. Images shown in TEM micrographs (Fig. 14) are not of COVID-19 virus but give Pd nanoparticles attached on the surface of lignin based phenolic nanospheres before catalysis (d and e) and after catalysis (a and b).

9. Conclusions and future directions

The purpose of this report was to present recent research development in designing, fabrication and stabilization of inorganic nanoparticles for Cr(VI) reduction to Cr(III) in aqueous medium. Nanoparticles of non-noble metals like zerovalent iron can reduce Cr(VI) to Cr(III) without any additional catalyst and reducing agent but instability, metal oxide layer formation around zerovalent nanoparticles and co-precipitation of Cr(III) and M(III) on the surface of metal nanoparticles are major drawbacks. Precious noble metal (Pd and Pt) nanoparticles catalyzed Cr(VI) reduction by formic acid have been widely reported in literature. Few reports are also available on catalytic Cr(VI) reduction to Cr(III) by formic acid in the presence of relatively low cost noble metal (Ag) nanoparticles but mechanistic pathway is different from Pt/Pd catalyzed reduction of Cr(III). Although Cr(VI) reduction to Cr(III) may be carried out using different reducing agents including CO, H_2, sodium format, sodium borohydride and oxalic acid. Formic acid has gained much attention due to its good stability, water solubility, good reducing ability, cost effectiveness, benign nature and acidic properties. Catalytic Cr(VI) reduction can be easily monitored by UV–vis spectrophotometry. Catalytic reduction of Cr(VI) to Cr(III) is a function of pH, catalyst dose and temperature of the medium. Catalytic Cr(VI) reduction to Cr(III) has been rarely reported in the presence of non-metallic nanoparticles. Sulfur nanoparticles have been recently reported as non-metal nanocatalysts for Cr(VI) reduction to Cr(III) as alternate of metallic nanocatalysts (Tripathi et al., 2018). Non-metallic nanoparticles other than sulfur may be synthesized and characterized for catalytic Cr(VI) reduction to Cr(III) and mechanism of catalysis by non-metallic nanoparticles may be explored in future studies. The role of nanoparticles stabilizer/support has not been properly described in the most of reported works on Cr(VI) reduction that may be the subject of future publications. Morphology of nanocatalysts has significant effect on their catalytic activity (Xu et al., 2006) but it has not been studied in case of catalytic Cr(VI) reduction. Study of effect of morphologies of nanocatalysts on catalytic reduction of Cr(VI) may be a fascinating subject of future studies. Core-shell bimetallic nanoparticles have been reported for catalytic Cr(VI) reduction (Li et al., 2019) but effect of shell thickness and core size and exchange of core metal by shell metal may an interesting subject of future studies. Transition metal like manganese, copper and cobalt etc. nanoparticles may be stabilized in suitable stabilizer for catalytic Cr(VI) reduction to Cr(III). Green methodologies may be developed for synthesis and stabilization of inorganic nanoparticles to be used as catalysts for reduction of Cr(VI). Plant extracted material may also replace conventional reducing agents used for reduction of Cr(VI) to Cr(III). Excessive use of Cr(VI) in various industrial processes in future will result in high concentration of Cr(VI) in waste water and soil. Use of Nanocatalysts should be extended towards real application of reductive removal of Cr(VI) from soil and waste water. Product of catalytic reduction of Cr(VI) is CO_2 which is a greenhouse gas. Catalytic reactor used for Cr(VI) conversion to Cr(III) can be combined with carbon capture and storage technology to stop release of CO_2 into the atmosphere.

Declaration of Competing Interest

The author declares no conflict of interest.

Acknowledgments

Authors are thankful to the Higher Education Commission Pakistan under National Research Program for Universities (No.20-3995/NRPU/R&D/HEC/14/1212) and University of the Punjab, Lahore, Pakistan under research for the fiscal year of 2019–2020 [No:/503/EST.I]) for financial support to perform this work. Ahmad Irfan would like to acknowledge the financial support of King Khalid University for research through a grant RCAMS/KKU/006-20 under the (Research Center for Advanced Materials Science) at King Khalid University, Kingdom of Saudi Arabia.

References

Akram, M.Y., Hameed, M.U., Akhtar, N., Ali, S., Maitlo, I., Zhu, X.-Q., Jun, N., 2019. Synthesis of high performance Ni3C-Ni decorated thermally expanded reduced graphene oxide (TErGO/Ni3C-Ni) nanocomposite: a stable catalyst for reduction of Cr (VI) and organic dyes. J. Hazard. Mater. 366, 723–731.

Ali, I., Gupta, V., 2006. Advances in water treatment by adsorption technology. Nat. Protoc. 1, 2661.

Ambika, S., Devasena, M., Nambi, I.M., 2016. Synthesis, characterization and performance of high energy ball milled meso-scale zero valent iron in Fenton reaction. J. Environ. Manage. 181, 847–855.

Bao, S., Liu, H., Liu, Y., Yang, W., Wang, Y., Yu, Y., Sun, Y., Li, K., 2020. Amino-functionalized graphene oxide-supported networked Pd–Ag nanowires as highly efficient catalyst for reducing Cr (VI) in industrial effluent by formic acid. Chemosphere, 127245.

Barrera-Díaz, C.E., Lugo-Lugo, V., Bilyeu, B., 2012. A review of chemical, electrochemical and biological methods for aqueous Cr (VI) reduction. J. Hazard. Mater. 223, 1–12.

Begum, R., Naseem, K., Farooqi, Z.H., 2016. A review of responsive hybrid microgels fabricated with silver nanoparticles: synthesis, classification, characterization and applications. J. Solgel Sci. Technol. 77, 497–515.

Begum, R., Farooqi, Z.H., Ahmed, E., Naseem, K., Ashraf, S., Sharif, A., Rehan, R., 2017. Catalytic reduction of 4-nitrophenol using silver nanoparticles-engineered poly (N-isopropylacrylamide-co-acrylamide) hybrid microgels. Appl. Organomet. Chem. 31, e3563.

Begum, R., Farooqi, Z.H., Naseem, K., Ali, F., Batool, M., Xiao, J., Irfan, A., 2018a. Applications of UV/Vis spectroscopy in characterization and catalytic activity of noble metal nanoparticles fabricated in responsive polymer microgels: a review. Crit. Rev. Anal. Chem. 48, 503–516.

Begum, R., Farooqi, Z.H., Butt, Z., Wu, Q., Wu, W., Irfan, A., 2018b. Engineering of responsive polymer based nano-reactors for facile mass transport and enhanced catalytic degradation of 4-nitrophenol. J. Environ. Sci. 72, 43–52.

Begum, R., Najeeb, J., Ahmad, G., Wu, W., Irfan, A., Al-Sehemi, A.G., Farooqi, Z.H., 2018. Synthesis and characterization of poly (N-isopropylmethacrylamide-co-acrylic acid) microgels for in situ fabrication and stabilization of silver nanoparticles for catalytic reduction of o-nitroaniline in aqueous medium. React. Funct. Polym. 132, 89–97.

Begum, R., Farooqi, Z.H., Aboo, A.H., Ahmed, E., Sharif, A., Xiao, J., 2019. Reduction of nitroarenes catalyzed by microgel-stabilized silver nanoparticles. J. Hazard. Mater. 377, 399–408.

Beller, H.R., Han, R., Karaoz, U., Lim, H., Brodie, E.L., 2013. Genomic and physiological characterization of the chromate-reducing, aquifer-derived firmicute Pelosinus sp. Strain HCF1. Appl. Environ. Microbiol. 79, 63–73.

Benazir, J.F., Suganthi, R., Rajvel, D., Pooja, M.P., Mathithumilan, B., 2010. Bioremediation of chromium in tannery effluent by microbial consortia. Afr. J. Biotechnol. 9, 3140–3143.

Bhowmik, K., Mukherjee, A., Mishra, M.K., De, G., 2014. Stable Ni nanoparticle–reduced graphene oxide composites for the reduction of highly toxic aqueous Cr (VI) at room temperature. Langmuir 30, 3209–3216.

Borah, B.J., Saikia, H., Bharali, P., 2014. Reductive conversion of Cr (VI) to Cr (III) over bimetallic CuNi nanocrystals at room temperature. New J. Chem. 38, 2748–2751.

Celebi, M., Yurderi, M., Bulut, A., Kaya, M., Zahmakiran, M., 2016. Palladium nanoparticles supported on amine-functionalized SiO_2 for the catalytic hexavalent chromium reduction. App. Catal. B: Environ. 180, 53–64.

Chen, C., Zhu, K., Chen, K., Alsaedi, A., Hayat, T., 2018. Synthesis of Ag nanoparticles decoration on magnetic carbonized polydopamine nanospheres for effective catalytic reduction of Cr (VI). J. Colloid Interface Sci. 526, 1–8.

Chen, Z., Wei, D., Li, Q., Wang, X., Yu, S., Liu, L., Liu, B., Xie, S., Wang, J., Chen, D., 2018. Macroscopic and microscopic investigation of Cr (VI) immobilization by nanoscaled zero-valent iron supported zeolite MCM-41 via batch, visual, XPS and EXAFS techniques. J. Cleaner Prod. 181, 745–752.

Chen, Y., Liang, W., Li, Y., Wu, Y., Chen, Y., Xiao, W., Zhao, L., Zhang, J., Li, H., 2019. Modification, application and reaction mechanisms of nano-sized iron sulfide particles for pollutant removal from soil and water: a review. Chem. Eng. J. 362, 144–159.

Chen, S., Wang, G., Sui, W., Parvez, A.M., Dai, L., Si, C., 2020. Novel lignin-based phenolic nanosphere supported palladium nanoparticles with highly efficient catalytic performance and good reusability. Ind. Crops Prod. 145, 112164.

Cheung, K., Gu, J.-D., 2007. Mechanism of hexavalent chromium detoxification by microorganisms and bioremediation application potential: a review. Int. Biodeterior. Biodegrad. 59, 8–15.

Costa, M., Klein, C.B., 2006. Toxicity and carcinogenicity of chromium compounds in humans. Crit. Rev. Toxicol. 36, 155–163.

Dandapat, A., Jana, D., De, G., 2011. Pd nanoparticles supported mesoporous γ-Al_2O_3 film as a reusable catalyst for reduction of toxic CrVI to CrIII in aqueous solution. App. Catal. A 396, 34–39.

Dandapat, A., Huang, Y., Gnayem, H., Sasson, Y., 2017. Bismuth oxyhalide induced growth of Pt nanoparticles within mesoporous alumina films and their use as reusable catalyst for chromium (VI) reduction. ChemistrySelect 2, 620–623.

Diao, Z.-H., Xu, X.-R., Jiang, D., Kong, L.-J., Sun, Y.-X., Hu, Y.-X., Hao, Q.-W., Chen, H., 2016. Bentonite-supported nanoscale zero-valent iron/persulfate system for the simultaneous removal of Cr (VI) and phenol from aqueous solutions. Chem. Eng. J. 302, 213–222.

Dorosti, M., Baghdadi, M., Nasimi, S., 2020. A continuous electroreduction cell composed of palladium nanocatalyst immobilized on discarded cigarette filters as an active bed for Cr (VI) removal from groundwater. J. Environ. Manage. 264, 110409.

Du, J., Bao, J., Lu, C., Werner, D., 2016. Reductive sequestration of chromate by hierarchical FeS@ Fe0 particles. Water Res. 102, 73–81.

Dumestre, F., Chaudret, B., Amiens, C., Renaud, P., Fejes, P., 2004. Superlattices of iron nanocubes synthesized from Fe [N (SiMe3) 2] 2. Science 303, 821–823.

Fazlzadeh, M., Rahmani, K., Zarei, A., Abdoallahzadeh, H., Nasiri, F., Khosravi, R., 2017. A novel green synthesis of zero valent iron nanoparticles (NZVI) using three plant extracts and their efficient application for removal of Cr (VI) from aqueous solutions. Adv. Powder Technol. 28, 122–130.

Fu, F., Ma, J., Xie, L., Tang, B., Han, W., Lin, S., 2013. Chromium removal using resin supported nanoscale zero-valent iron. J. Environ. Manage. 128, 822–827.

Gao, Y., Sun, W., Yang, W., Li, Q., 2018. Palladium nanoparticles supported on amine-functionalized glass fiber mat for fixed-bed reactors on the effective removal of hexavalent chromium by catalytic reduction. J. Mater. Sci. Technol. 34, 961–968.

Gheju, M., 2011. Hexavalent chromium reduction with zero-valent iron (ZVI) in aquatic systems. Water Air Soil Pollut. 222, 103–148.

Gheju, M., 2017. Decontamination of hexavalent chromium-polluted waters: significance of metallic iron technology. Enhancing Cleanup of Environmental Pollutants. Springer, pp. 209–253.

Gheju, M., 2018. Progress in understanding the mechanism of CrVI Removal in Fe0-based filtration systems. Water 10, 651.

Golbaz, S., Jafari, A.J., Rafiee, M., Kalantary, R.R., 2014. Separate and simultaneous removal of phenol, chromium, and cyanide from aqueous solution by coagulation/precipitation: mechanisms and theory. Chem. Eng. J. 253, 251–257.

Gong, K., Wang, W., Yan, J., Han, Z., 2015. Highly reduced molybdophosphate as a noble-metal-free catalyst for the reduction of chromium using formic acid as a reducing agent. J. Mater. Chem. A 3, 6019–6027.

Gong, Y., Tang, J., Zhao, D., 2016. Application of iron sulfide particles for groundwater and soil remediation: a review. Water Res. 89, 309–320.

Gong, Y., Gai, L., Tang, J., Fu, J., Wang, Q., Zeng, E.Y., 2017. Reduction of Cr (VI) in simulated groundwater by FeS-coated iron magnetic nanoparticles. Sci. Total Environ. 595, 743–751.

González-Arellano, C., Campelo, J.M., Macquarrie, D.J., Marinas, J.M., Romero, A.A., Luque, R., 2008. Efficient microwave oxidation of alcohols using low-loaded supported metallic iron nanoparticles. ChemSusChem Chem. Sustain. Energy Mater. 1, 746–750.

Hisano, S., Saito, K., 1998. Research and development of metal powder for magnetic recording. J. Magn. Magn. Mater. 190, 371–381.

Hoeppener, S., Maoz, R., Cohen, S.R., Chi, L., Fuchs, H., Sagiv, J., Nanoparticles, Metal, 2002. Nanowires, and contact electrodes self-assembled on patterned monolayer templates—a bottom-up chemical approach. Adv. Mater. 14, 1036–1041.

Hu, C.-Y., Lo, S.-L., Liou, Y.-H., Hsu, Y.-W., Shih, K., Lin, C.-J., 2010. Hexavalent chromium removal from near natural water by copper–iron bimetallic particles. Water Res. 44, 3101–3108.

Hu, L.-Y., Chen, L.-X., Liu, M.-T., Wang, A.-J., Wu, L.-J., Feng, J.-J., 2017. Theophylline-assisted, eco-friendly synthesis of PtAu nanospheres at reduced graphene oxide with enhanced catalytic activity towards Cr (VI) reduction. J. Colloid Interface Sci. 493, 94–102.

Hu, Y., Peng, X., Ai, Z., Jia, F., Zhang, L., 2019. Liquid nitrogen activation of zero-valent iron and its enhanced Cr (VI) removal performance. Environ. Sci. Tech. 53, 8333–8341.

Huang, Y., Ma, H., Wang, S., Shen, M., Guo, R., Cao, X., Zhu, M., Shi, X., 2012. Efficient catalytic reduction of hexavalent chromium using palladium nanoparticle-immobilized electrospun polymer nanofibers. ACS Appl. Mater. Interfaces 4, 3054–3061.

Jiang, D., Huang, D., Lai, C., Xu, P., Zeng, G., Wan, J., Tang, L., Dong, H., Huang, B., Hu, T., 2018. Difunctional chitosan-stabilized Fe/Cu bimetallic nanoparticles for removal of hexavalent chromium wastewater. Sci. Total Environ. 644, 1181–1189.

Jin, X., Liu, Y., Tan, J., Owens, G., Chen, Z., 2018. Removal of Cr (VI) from aqueous solutions via reduction and absorption by green synthesized iron nanoparticles. J. Cleaner Prod. 176, 929–936.

Jobby, R., Jha, P., Yadav, A.K., Desai, N., 2018. Biosorption and biotransformation of hexavalent chromium [Cr (VI)]: a comprehensive review. Chemosphere 207, 255–266.

Kadu, B.S., Sathe, Y.D., Ingle, A.B., Chikate, R.C., Patil, K.R., Rode, C.V., 2011. Efficiency and recycling capability of montmorillonite supported Fe–Ni bimetallic

nanocomposites towards hexavalent chromium remediation. App. Catal. B: Environ. 104, 407–414.
Kalwar, N.H., Uddin, S., Sherazi, S.T.H., Khaskheli, A.R., Shah, A., 2013. Reduction of hexavalent chromium using l-cysteine capped nickel nanocatalysts. Pak. J. Anal. Environ. Chem.14 7.
Katz, S.A., Salem, H., 1993. The toxicology of chromium with respect to its chemical speciation: a review. J. Appl. Toxicol. 13, 217–224.
Kaya, A., Onac, C., Alpoguz, H.K., Yilmaz, A., Atar, N., 2016. Removal of Cr (VI) through calixarene based polymer inclusion membrane from chrome plating bath water. Chem. Eng. J. 283, 141–149.
Li, Y., Jin, Z., Li, T., Xiu, Z., 2012. One-step synthesis and characterization of core–shell Fe@ SiO2 nanocomposite for Cr (VI) reduction. Sci.Total Environ. 421, 260–266.
Li, X., Ai, L., Jiang, J., 2016a. Nanoscale zerovalent iron decorated on graphene nanosheets for Cr (VI) removal from aqueous solution: surface corrosion retard induced the enhanced performance. Chem. Eng. J. 288, 789–797.
Li, H.-C., Liu, W.-J., Han, H.-X., Yu, H.-Q., 2016b. Hydrophilic swellable metal–organic framework encapsulated Pd nanoparticles as an efficient catalyst for Cr (VI) reduction. J. Mater. Chem. A 4, 11680–11687.
Li, S., Tang, L., Zeng, G., Wang, J., Deng, Y., Wang, J., Xie, Z., Zhou, Y., 2016. Catalytic reduction of hexavalent chromium by a novel nitrogen-functionalized magnetic ordered mesoporous carbon doped with Pd nanoparticles. Environ. Sci. Pollut. Res. 23, 22027–22036.
Li, Y., Wang, W., Zhou, L., Liu, Y., Mirza, Z.A., Lin, X., 2017. Remediation of hexavalent chromium spiked soil by using synthesized iron sulfide particles. Chemosphere 169, 131–138.
Li, D.-N., Shao, F.-Q., Feng, J.-J., Wei, J., Zhang, Q.-L., Wang, A.-J., 2018. Uniform Pt@ Pd nanocrystals supported on N-doped reduced graphene oxide as catalysts for effective reduction of highly toxic chromium (VI). Mater. Chem. Phys. 205, 64–71.
Li, X., Li, C., Xiang, D., Zhang, C., Xia, L., Liu, X., Zheng, F., Xie, X., Zhang, Y., Chen, W., 2019. Self-limiting synthesis of Au–Pd core–shell nanocrystals with a near surface alloy and monolayer Pd shell structure and their superior catalytic activity on the conversion of hexavalent chromium. App. Catal. B: Environ. 253, 263–270.
Liang, M., Su, R., Qi, W., Zhang, Y., Huang, R., Yu, Y., Wang, L., He, Z., 2014. Reduction of hexavalent chromium using recyclable Pt/Pd nanoparticles immobilized on procyanidin-grafted eggshell membrane. Ind. Eng. Chem. Res. 53, 13635–13643.
Liu, W.-J., Qian, T.-T., Jiang, H., 2014. Bimetallic Fe nanoparticles: recent advances in synthesis and application in catalytic elimination of environmental pollutants. Chem. Eng. J. 236, 448–463.
Liu, W.-J., Ling, L., Wang, Y.-Y., He, H., He, Y.-R., Yu, H.-Q., Jiang, H., 2016a. One-pot high yield synthesis of Ag nanoparticle-embedded biochar hybrid materials from waste biomass for catalytic Cr (VI) reduction. Environ. Sci. Nano 3, 745–753.
Liu, Q., Xu, M., Li, F., Wu, T., Li, Y., 2016. Rapid and effective removal of Cr (VI) from aqueous solutions using the $FeCl_3$/$NaBH_4$ system. Chem. Eng. J. 296, 340–348.
Lu, H., Tian, B., Wang, J., Hao, H., 2017. Montmorillonite-supported Fe/Ni bimetallic nanoparticles for removal of Cr (VI) from wastewater. Chem. Eng. Trans. 60, 169–174.
Lv, X., Xu, J., Jiang, G., Xu, X., 2011. Removal of chromium (VI) from wastewater by nanoscale zero-valent iron particles supported on multiwalled carbon nanotubes. Chemosphere 85, 1204–1209.
Lv, X., Jiang, G., Xue, X., Wu, D., Sheng, T., Sun, C., Xu, X., 2013. Fe^0-Fe_3O_4 nanocomposites embedded polyvinyl alcohol/sodium alginate beads for chromium (VI) removal. J. Hazard. Mater. 262, 748–758.
Lv, X., Xue, X., Jiang, G., Wu, D., Sheng, T., Zhou, H., Xu, X., 2014. Nanoscale zero-valent iron (nZVI) assembled on magnetic Fe_3O_4/graphene for chromium (VI) removal from aqueous solution. J. Colloid Interface Sci. 417, 51–59.
Lv, X., Zhang, Y., Fu, W., Cao, J., Zhang, J., Ma, H., Jiang, G., 2017. Zero-valent iron nanoparticles embedded into reduced graphene oxide-alginate beads for efficient chromium (VI) removal. J. Colloid Interface Sci. 506, 633–643.
Lv, Z., Tan, X., Wang, C., Alsaedi, A., Hayat, T., Chen, C., 2020. Metal-organic frameworks-derived 3D yolk shell-like structure Ni@ carbon as a recyclable catalyst for Cr (VI) reduction. Chem. Eng. J. 389, 123428.
Lyu, H., Tang, J., Huang, Y., Gai, L., Zeng, E.Y., Liber, K., Gong, Y., 2017. Removal of hexavalent chromium from aqueous solutions by a novel biochar supported nanoscale iron sulfide composite. Chem. Eng. J. 322, 516–524.
Lyu, H., Zhao, H., Tang, J., Gong, Y., Huang, Y., Wu, Q., Gao, B., 2018. Immobilization of hexavalent chromium in contaminated soils using biochar supported nanoscale iron sulfide composite. Chemosphere 194, 360–369.
Mahar, A.M., Balouch, A., Talpur, F.N., Kumar, A., Panah, P., Shah, M.T., 2019. Synthesis and catalytic applicability of Pt–Pd ITO grown nano catalyst: an excellent candidate for reduction of toxic hexavalent chromium. Catal. Lett. 149, 2415–2424.
Mai, Z., Hu, Y., Huang, P., Zhang, X., Dong, X., Fang, Y., Wu, C., Cheng, J., Zhou, W., 2017. Outside-in stepwise bi-functionalization of magnetic mesoporous silica incorporated with Pt nanoparticles for effective removal of hexavalent chromium. Powder Technol. 312, 48–57.
Maitlo, H.A., Kim, K.-H., Kumar, V., Kim, S., Park, J.-W., 2019. Nanomaterials-based treatment options for chromium in aqueous environments. Environ. Int. 130, 104748.
Malaviya, P., Singh, A., 2011. Physicochemical technologies for remediation of chromium-containing waters and wastewaters. Crit. Rev. Environ. Sci. Technol. 41, 1111–1172.
Maponya, T.C., Ramohlola, K.E., Kera, N.H., Modibane, K.D., Maity, A., Katata-Seru, L. M., Hato, M.J., 2020. Influence of magnetic nanoparticles on modified polypyrrole/m-phenylediamine for adsorption of Cr (VI) from aqueous solution. Polym. 12, 679.
Miretzky, P., Cirelli, A.F., 2010. Cr (VI) and Cr (III) removal from aqueous solution by raw and modified lignocellulosic materials: a review. J. Hazard. Mater. 180, 1–19.
Naseem, K., Farooqi, Z.H., Begum, R., Irfan, A., 2018. Removal of Congo red dye from aqueous medium by its catalytic reduction using sodium borohydride in the presence of various inorganic nano-catalysts: a review. J. Cleaner Prod. 187, 296–307.
Naseem, K., Begum, R., Wu, W., Irfan, A., Al-Sehemi, A.G., Farooqi, Z.H., 2019. Catalytic reduction of toxic dyes in the presence of silver nanoparticles impregnated core-shell composite microgels. J. Cleaner Prod. 211, 855–864.
Nasrollahzadeh, M., Bidgoli, N.S.S., Issaabadi, Z., Ghavamifar, Z., Baran, T., Luque, R., 2020. Hibiscus Rosasinensis L. Aqueous extract-assisted valorization of lignin: preparation of magnetically reusable Pd NPs@ Fe_3O_4-lignin for Cr (VI) reduction and Suzuki-Miyaura reaction in eco-friendly media. Int. J. Biol. Macromol. 148, 265–275.
Ng, C.K., Karahan, H.E., Loo, S.C.J., Chen, Y., Cao, B., 2019. Biofilm-templated heteroatom-doped carbon–Palladium nanocomposite catalyst for hexavalent chromium reduction. ACS Appl. Mater. Interfaces 11, 24018–24026.
Okazoe, S., Yasaka, Y., Kudo, M., Maeno, H., Murakami, Y., Kimura, Y., 2018. Synthesis of zero-valent iron nanoparticles via laser ablation in a formate ionic liquid under atmospheric conditions. Chem. Commun. 54, 7834–7837.
Omole, M.A., K'Owino, I.O., Sadik, O.A., 2007. Palladium nanoparticles for catalytic reduction of Cr (VI) using formic acid. App. Catal. B: Environ. 76, 158–167.
Peng, X., Pan, Q., Rempel, G.L., 2008. Bimetallic dendrimer-encapsulated nanoparticles as catalysts: a review of the research advances. Chem. Soc. Rev. 37, 1619–1628.
Petala, E., Dimos, K., Douvalis, A., Bakas, T., Tucek, J., Zbořil, R., Karakassides, M.A., 2013. Nanoscale zero-valent iron supported on mesoporous silica: characterization and reactivity for Cr (VI) removal from aqueous solution. J. Hazard. Mater. 261, 295–306.
Qian, L., Zhang, W., Yan, J., Han, L., Chen, Y., Ouyang, D., Chen, M., 2017. Nanoscale zero-valent iron supported by biochars produced at different temperatures: synthesis mechanism and effect on Cr (VI) removal. Environ. Pollut. 223, 153–160.
Rai, M., Ingle, A.P., Paralikar, P., 2016. Sulfur and sulfur nanoparticles as potential antimicrobials: from traditional medicine to nanomedicine. Expert Rev. Anti-Infect. Ther. 14, 969–978.
Ravikumar, K., Santhosh, S., Sudakaran, S.V., Nancharaiah, Y.V., Mrudula, P., Chandrasekaran, N., Mukherjee, A., 2018. Biogenic nano zero valent iron (Bio-nZVI) anaerobic granules for textile dye removal. J. Environ. Chem. Eng. 6, 1683–1689.
Ruan, X., Liu, H., Ning, X., Zhao, D., Fan, X., 2020. Screening for the action mechanisms of Fe and Ni in the reduction of Cr (VI) by Fe/Ni nanoparticles. Sci. Total Environ. 715, 136822.
Sadeghi, I., Liu, E.Y., Yi, H., Asatekin, A., 2019. Membranes with thin hydrogel selective layers containing viral-templated palladium nanoparticles for the catalytic reduction of Cr (VI) to Cr (III). ACS Appl. Nano Mater. 2, 5233–5244.
Sadik, O.A., Noah, N.M., Okello, V.A., Sun, Z., 2014. Catalytic reduction of hexavalent chromium using palladium nanoparticles: an undergraduate nanotechnology laboratory. J. Chem. Educ. 91, 269–273.
Saikia, H., Borah, B.J., Yamada, Y., Bharali, P., 2017. Enhanced catalytic activity of CuPd alloy nanoparticles towards reduction of nitroaromatics and hexavalent chromium. J. Colloid Interface Sci. 486, 46–57.
Sankar, M., Dimitratos, N., Miedziak, P.J., Wells, P.P., Kiely, C.J., Hutchings, G.J., 2012. Designing bimetallic catalysts for a green and sustainable future. Chem. Soc. Rev. 41, 8099–8139.
Shang, J., Zong, M., Yu, Y., Kong, X., Du, Q., Liao, Q., 2017. Removal of chromium (VI) from water using nanoscale zerovalent iron particles supported on herb-residue biochar. J. Environ. Manage. 197, 331–337.
Shao, F.-Q., Feng, J.-J., Lin, X.-X., Jiang, L.-Y., Wang, A.-J., 2017. Simple fabrication of AuPd@ Pd core-shell nanocrystals for effective catalytic reduction of hexavalent chromium. App. Catal. B: Environ. 208, 128–134.
Shao-feng, N., Yong, L., Xin-Hua, X., Zhang-hua, L., 2005. Removal of hexavalent chromium from aqueous solution by iron nanoparticles. J. Zhejiang Univ. Sci. 6, 1022–1027.
Shi, L.-n., Lin, Y.-M., Zhang, X., Chen, Z.-l., 2011. Synthesis, characterization and kinetics of bentonite supported nZVI for the removal of Cr (VI) from aqueous solution. Chem. Eng. J. 171, 612–617.
Shi, D., Ouyang, Z., Zhao, Y., Xiong, J., Shi, X., 2019. Catalytic reduction of hexavalent chromium using Iron/Palladium bimetallic nanoparticle-assembled filter paper. Nanomaterials 9, 1183.
Sivaranjan, K., Santhanalakshmi, J., Panneer, D.S., Vivekananthan, S., Sagadevan, S., Johan, M., Bin, R., Anita Lett, J., Hegazy, H., Umar, A., 2020. Synthesis of Iron oxide@ Pt core–Shell nanoparticles for reductive conversion of Cr (VI) to Cr (III) and antibacterial studies. J. Nanosci. Nanotechnol. 20, 918–923.
Stefaniuk, M., Oleszczuk, P., Ok, Y.S., 2016. Review on nano zerovalent iron (nZVI): from synthesis to environmental applications. Chem. Eng. J. 287, 618–632.
Su, H., Fang, Z., Tsang, P.E., Zheng, L., Cheng, W., Fang, J., Zhao, D., 2016. Remediation of hexavalent chromium contaminated soil by biochar-supported zero-valent iron nanoparticles. J. Hazard. Mater. 318, 533–540.
Suleiman, M., Al Ali, A., Hussein, A., Hammouti, B., Hadda, T.B., Warad, I., 2013. Sulfur nanoparticles: synthesis, characterizations and their applications. J. Mater. Environ. Sci. 4, 1029–1033.
Sun, T.R., Pamukcu, S., Ottosen, L.M., Wang, F., 2015. Electrochemically enhanced reduction of hexavalent chromium in contaminated clay: kinetics, energy consumption, and application of pulse current. Chem. Eng. J. 262, 1099–1107.
Tan, H., Wang, C., Li, H., Peng, D., Zeng, C., Xu, H., 2020. Remediation of hexavalent chromium contaminated soil by nano-FeS coated humic acid complex in combination with Cr-resistant microflora. Chemosphere 242, 125251.
Tian, X., Liu, M., Iqbal, K., Ye, W., Chang, Y., 2020. Facile synthesis of nitrogen-doped carbon coated Fe_3O_4/Pd nanoparticles as a high-performance catalyst for Cr (VI) reduction. J. Alloys. Compd. 826, 154059.

Tripathi, R., Chung, S.J., 2020. Reclamation of hexavalent chromium using catalytic activity of highly recyclable biogenic Pd (0) nanoparticles. Sci. Rep. 10, 1–14.
Tripathi, R., Rao, R.P., Tsuzuki, T., 2018. Green synthesis of sulfur nanoparticles and evaluation of their catalytic detoxification of hexavalent chromium in water. RSC Adv. 8, 36345–36352.
Trivedi, M., Kumar, A., Singh, G., Kumar, A., Rath, N.P., 2016. Metal–organic framework MIL-101 supported bimetallic Pd–Cu nanocrystals as efficient catalysts for chromium reduction and conversion of carbon dioxide at room temperature. New J. Chem. 40, 3109–3118.
Veerakumar, P., Lin, K.-C., 2020. An overview of palladium supported on carbon-based materials: synthesis, characterization, and its catalytic activity for reduction of hexavalent chromium. Chemosphere, 126750.
Veerakumar, P., Thanasekaran, P., Lin, K.-C., Liu, S.-B., 2017. Biomass derived sheet-like carbon/palladium nanocomposite: an excellent opportunity for reduction of toxic hexavalent chromium. ACS Sustainable Chem. Eng. 5, 5302–5312.
Vellaichamy, B., Periakaruppan, P., 2016. A facile, one-pot and eco-friendly synthesis of gold/silver nanobimetallics smartened rGO for enhanced catalytic reduction of hexavalent chromium. RSC Adv. 6, 57380–57388.
Venkateswaran, P., Palanivelu, K., 2004. Solvent extraction of hexavalent chromium with tetrabutyl ammonium bromide from aqueous solution. Sep. Purif. Technol. 40, 279–284.
Vollmer, C., Janiak, C., 2011. Naked metal nanoparticles from metal carbonyls in ionic liquids: easy synthesis and stabilization. Coord. Chem. Rev. 255, 2039–2057.
Wang, X.B., Liu, J., Zhao, D.L., Song, X.J., 2011. Preparation of CMC-stabilized FeS Nanoparticles and Their Enhanced Performance for Cr (VI) Removal. Adv. Mater. Res. Trans Tech Publ, pp. 96–99.
Wang, C.-C., Du, X.-D., Li, J., Guo, X.-X., Wang, P., Zhang, J., 2016. Photocatalytic Cr (VI) reduction in metal-organic frameworks: a mini-review. App. Catal. B: Environ. 193, 198–216.
Wang, R., Jing, G., Zhou, X., Lv, B., 2017. Removal of chromium (VI) from wastewater by Mg-aminoclay coated nanoscale zero-valent iron. J. water process Eng. 18, 134–143.
Wang, Z., Yang, J., Li, Y., Zhuang, Q., Gu, J., 2018. In situ carbothermal synthesis of nanoscale zero-valent Iron functionalized porous carbon from metal–Organic frameworks for efficient detoxification of chromium (VI). Eur. J. Inorg. Chem. 2018, 23–30.
Wang, T., Liu, Y., Wang, J., Wang, X., Liu, B., Wang, Y., 2019. In-situ remediation of hexavalent chromium contaminated groundwater and saturated soil using stabilized iron sulfide nanoparticles. J. Environ. Manage. 231, 679–686.
Wei, L.-L., Gu, R., Lee, J.-M., 2015. Highly efficient reduction of hexavalent chromium on amino-functionalized palladium nanowires. App. Catal. B: Environ. 176, 325–330.
Wu, Y., Zhang, J., Tong, Y., Xu, X., 2009. Chromium (VI) reduction in aqueous solutions by Fe3O4-stabilized Fe0 nanoparticles. J. Hazard. Mater. 172, 1640–1645.
Wu, J., Wang, X.-B., Zeng, R.J., 2017. Reactivity enhancement of iron sulfide nanoparticles stabilized by sodium alginate: taking Cr (VI) removal as an example. J. Hazard. Mater. 333, 275–284.
Wu, H., Li, L., Chang, K., Du, K., Shen, C., Zhou, S., Sheng, G., Linghu, W., Hayat, T., Guo, X., 2020. Graphene oxide decorated nanoscale iron sulfide for highly efficient scavenging of hexavalent chromium from aqueous solutions. J. Environ. Chem. Eng., 103882
Xiao, K., Xu, F., Jiang, L., Duan, N., Zheng, S., 2016. Resin oxidization phenomenon and its influence factor during chromium (VI) removal from wastewater using gel-type anion exchangers. Chem. Eng. J. 283, 1349–1356.
Xu, R., Wang, D., Zhang, J., Li, Y., 2006. Shape-dependent catalytic activity of silver nanoparticles for the oxidation of styrene. Chemistry–An Asian J. 888–893.
Yadav, M., Xu, Q., 2013. Catalytic chromium reduction using formic acid and metal nanoparticles immobilized in a metal–organic framework. Chem. Commun. 49, 3327–3329.
Yang, C., Manocchi, A.K., Lee, B., Yi, H., 2010. Viral templated palladium nanocatalysts for dichromate reduction. App. Catal. B: Environ. 93, 282–291.
Yang, C., Meldon, J.H., Lee, B., Yi, H., 2014. Investigation on the catalytic reduction kinetics of hexavalent chromium by viral-templated palladium nanocatalysts. Catal. Today 233, 108–116.
Yao, D., Xu, T., Yuan, J., Tao, Y., He, G., Chen, H., 2020. Graphene based copper-nickel bimetal nanocomposite: magnetically separable catalyst for reducing hexavalent chromium. ChemistrySelect 5, 3243–3247.
Yi, Y., Tu, G., Zhao, D., Tsang, P.E., Fang, Z., 2020. Key role of FeO in the reduction of Cr (VI) by magnetic biochar synthesised using steel pickling waste liquor and sugarcane bagasse. J. Cleaner Prod. 245, 118886.
Yu, Y.-Y., Cheng, Q.-W., Sha, C., Chen, Y.-X., Naraginti, S., Yong, Y.-C., 2020. Size-controlled biosynthesis of FeS nanoparticles for efficient removal of aqueous Cr (VI). Chem. Eng. J. 379, 122404.
Zhang, H., Wang, T., Wang, J., Liu, H., Dao, T.D., Li, M., Liu, G., Meng, X., Chang, K., Shi, L., 2016. Surface-plasmon-enhanced photodriven CO2 reduction catalyzed by metal–organic-framework-derived iron nanoparticles encapsulated by ultrathin carbon layers. Adv. Mater. 28, 3703–3710.
Zhang, Z., Sun, L., Liu, R., 2018. Flash nanoprecipitation of polymer supported Pt colloids with tunable catalytic chromium reduction property. Colloid Polym. Sci. 296, 327–333.
Zhang, S., Lyu, H., Tang, J., Song, B., Zhen, M., Liu, X., 2019. A novel biochar supported CMC stabilized nano zero-valent iron composite for hexavalent chromium removal from water. Chemosphere 217, 686–694.
Zhao, X., Liu, W., Cai, Z., Han, B., Qian, T., Zhao, D., 2016. An overview of preparation and applications of stabilized zero-valent iron nanoparticles for soil and groundwater remediation. Water Res. 100, 245–266.
Zhao, S., Chen, Z., Shen, J., Qu, Y., Wang, B., Wang, X., 2017. Enhanced Cr (VI) removal based on reduction-coagulation-precipitation by NaBH4 combined with fly ash leachate as a catalyst. Chem. Eng. J. 322, 646–656.
Zhao, M., Zhang, C., Yang, X., Liu, L., Wang, X., Yin, W., Li, Y.C., Wang, S., Fu, W., 2020. Preparation of highly-conductive pyrogenic carbon-supported zero-valent iron for enhanced Cr (VI) reduction. J. Hazard. Mater. 122712.
Zhou, X., Jing, G., Lv, B., Zhou, Z., Zhu, R., 2016. Highly efficient removal of chromium (VI) by Fe/Ni bimetallic nanoparticles in an ultrasound-assisted system. Chemosphere 160, 332–341.
Zhou, N., Gong, K., Hu, Q., Cheng, X., Zhou, J., Dong, M., Wang, N., Ding, T., Qiu, B., Guo, Z., 2020. Optimizing nanocarbon shell in zero-valent iron nanoparticles for improved electron utilization in Cr (VI) reduction. Chemosphere 242, 125235.
Zhu, K., Chen, C., Lu, S., Zhang, X., Alsaedi, A., Hayat, T., 2019. MOFs-induced encapsulation of ultrafine Ni nanoparticles into 3D N-doped graphene-CNT frameworks as a recyclable catalyst for Cr (VI) reduction with formic acid. Carbon 148, 52–63.